

Supporting information for

Engineering BODIPY-based near-infrared nanoparticles with large Stokes shifts and aggregation-induced emission characteristics for organelle specific bioimaging

Xing Guo,[†] Bing Tang,[†] Qinghua Wu,^{*,‡} Weibin Bu,[†] Fan Zhang,[†] Changjiang Yu,[†] Lijuan Jiao[†] and Erhong Hao^{*,†}

[†]*The Key Laboratory of Functional Molecular Solids, Ministry of Education; College of Chemistry and Materials Science, Anhui Normal University, Wuhu 241002, China.*

[‡]*School of Pharmacy, Anhui University of Chinese Medicine, Hefei 230012, China*

Email: qinghuaw@ahctm.edu.cn, haoehong@ahnu.edu.cn

Contents

1. Photophysical Spectra	S2
2. Theoretical Calculation	S7
3. Cytotoxicity Studies	S14
4. Cellular Fluorescence Imaging	S15
5. ¹ H NMR, ¹³ C NMR and HRMS spectra for TPAB and 2TPAB	S29
6. References	S33

1. Photophysical Spectra

Table S1. Photophysical properties and fluorescent lifetimes of **TPAB**, **2TPAB** and **mes-BDP** in solution at room temperature.

dyes	solvent	$\lambda_{\text{abs}}^{\text{max}}$ [nm]	$\lambda_{\text{em}}^{\text{max}}$ [nm]	Φ^{a}	Stokes shift [nm]	Stokes shift [cm ⁻¹]	τ^{b} [ns]	k_f^{c} [$\times 10^8 \text{ s}^{-1}$]	K_{nr}^{d} [$\times 10^8 \text{ s}^{-1}$]
TPAB	hexane	588	618	0.96	30	830	4.93	1.95	0.08
	toluene	597	650	0.96	53	1370	4.55	2.11	0.09
	CHCl ₃	594	700	0.70	106	2550	4.37	1.60	0.69
	CH ₂ Cl ₂	589	736	0.13	147	3390	4.5	0.29	1.93
	THF	589	714	0.27	125	2970	3.94	0.69	1.85
	CH ₃ OH	582	730	0.006	148	3480	0.78	0.08	12.74
	CH ₃ CN	581	755	0.002	174	3970	0.81	0.02	12.32
2TPAB	hexane	640	692	0.83	52	1170	5.58	1.49	0.30
	toluene	650	711	0.75	61	1320	5.02	1.49	0.50
	CHCl ₃	648	724	0.75	76	1620	5.38	1.39	0.46
	CH ₂ Cl ₂	644	736	0.65	92	1940	4.82	1.35	0.73
	THF	647	720	0.65	73	1570	4.74	1.37	0.74
	CH ₃ OH	637	730	0.76	93	2000	0.88	8.64	2.73
	CH ₃ CN	637	753	0.03	116	2420	0.88	0.39	10.98
mes-BDP	hexane	498	511	0.99	13	510	7.72	1.28	0.01
	toluene	503	517	0.99	14	540	6.65	1.52	0.02
	CH ₂ Cl ₂	500	514	0.90	14	540	7.70	1.19	0.13
	CH ₃ CN	497	511	0.99	14	550	8.29	1.19	0.01

^aFluorescence quantum yields of **TPAB** and **2TPAB** were calculated using Cresyl Violet perchlorate ($\Phi = 0.54$ in methanol)¹ as the reference. Fluorescence quantum yields of **mes-BDP** was calculated using fluorescein ($\Phi = 0.92$ in 0.1 M NaOH solution)² as the reference. ^b τ = lifetime of different solution. ^c $k_f = \Phi/\tau$. ^d $k_{nr} = k_f * (1/\Phi - 1)$.

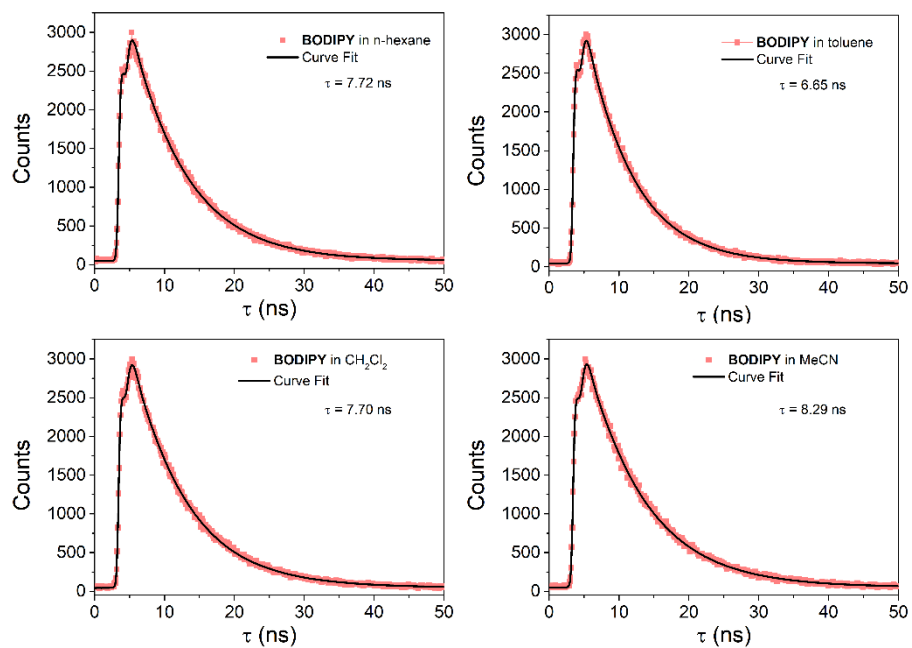


Figure S1. Fluorescence lifetime of **mes-BDP** in different solvents (n-hexane, toluene, CH_2Cl_2 , acetonitrile).

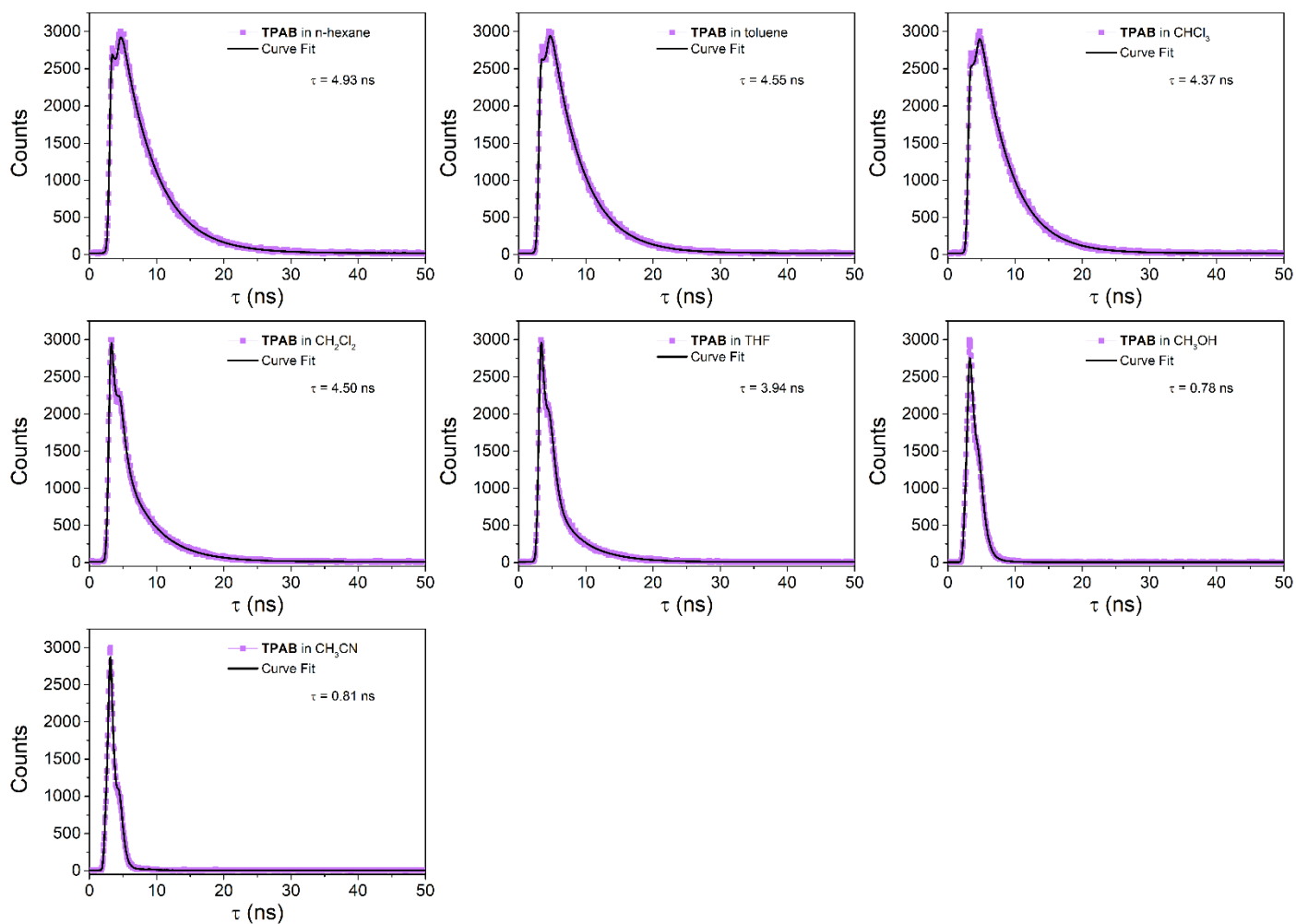


Figure S2. Fluorescence lifetime of **TPAB** in different solvents (n-hexane, toluene, CHCl_3 , CH_2Cl_2 , tetrahydrofuran, methanol, acetonitrile).

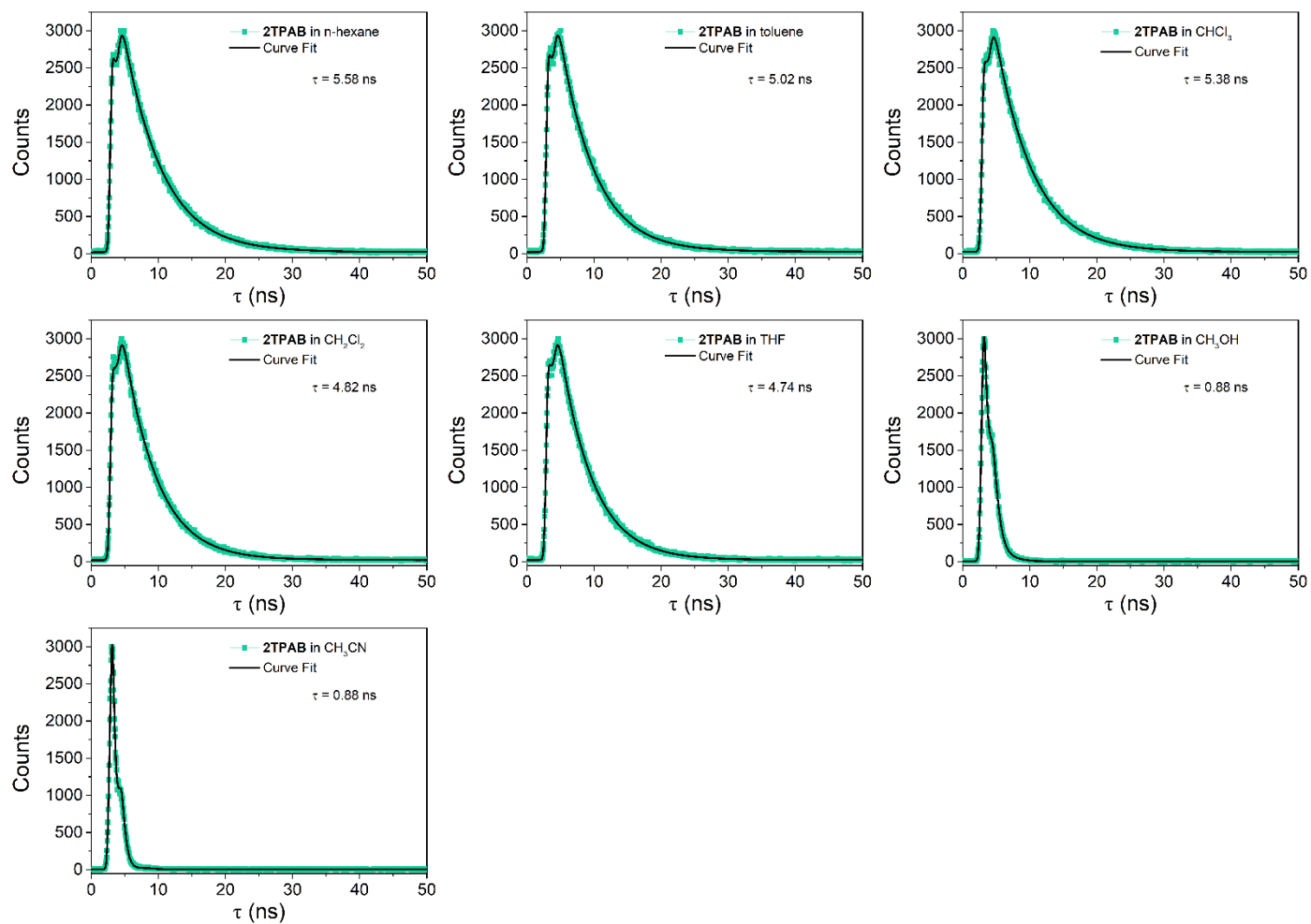


Figure S3. Fluorescence lifetime of **2TPAB** in different solvents (n-hexane, toluene, CHCl_3 , CH_2Cl_2 , tetrahydrofuran, methanol, acetonitrile).

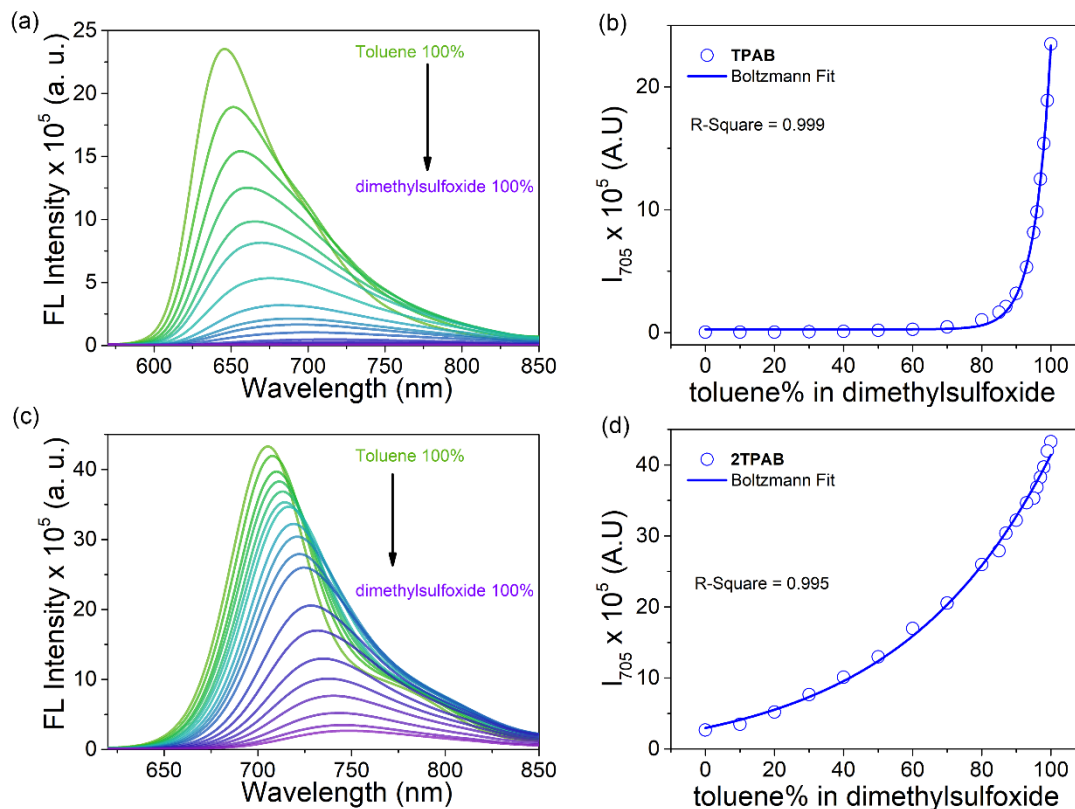


Figure S4. (a, c) Emission spectra of **TPAB/2TPAB** (5 μM) in mixture solvent with various toluene/dimethylsulfoxide ratios and (b, d) its exponential decay of fluorescence intensity denoting fluorogenic properties.

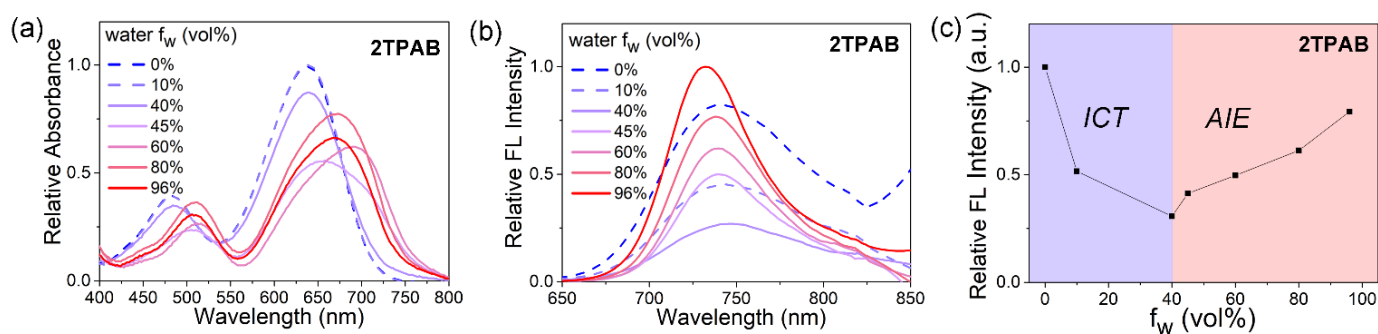


Figure S5. Relative absorption (a) and fluorescence (b) spectra of **2TPAB** (10 μM) in acetonitrile/deionized water with different water fractions (f_w); λ_{ex} : 600 nm. (c) Plot of the fluorescent intensity integration area versus different water fractions.

2. Theoretical Calculation

The ground state geometry was optimized by using DFT method at B3LYP/6-31G(d) level. The same method was adopted for vibrational analysis to verify that the optimized structures correspond to local minima on the energy surface. TD-DFT computations were used the optimized ground state geometries under the B3LYP/6-31+G(d,p) theoretical level. The molecule calculation in dichloromethane were using the Self-Consistent Reaction Field (SCRF) method and Polarizable Continuum Model (PCM). All of the calculations for **mes-BODIPY**, **TPAB** and **2TPAB** were carried out by the methods implemented in Gaussian 09 package.²

Table S2. Molecular orbital amplitude plots of HOMO and LUMO energy levels of **mes-BDP**, **TPAB** and **2TPAB** at the B3LYP/6-31G(d, p) level by using the Gaussian 09 program package.

	Electronic transition	TD//B3LYP/6-31G(d, p)			
		Energy/ eV ^[a]	f ^[b]	Composition ^[c]	CI ^[d]
mes-BDP	S0→S1	2.9534 eV 419.81 nm	0.0007	HOMO -1 → LUMO	0.7043
	S0→S2	3.0161 eV 411.08 nm	0.4495	HOMO -2 → LUMO	0.1832
				HOMO → LUMO	0.6790
	S0→S3	3.0994 eV 400.03 nm	0.0115	HOMO -1 → LUMO	0.7001
TPAB	S0→S1	2.0556 eV 603.16 nm	0.6464	HOMO → LUMO	0.7045
	S0→S2	2.8896 eV 429.06 nm	0.3832	HOMO -1 → LUMO	0.6899
2TPAB	S0→S1	1.8588 eV 667.02 nm	0.5636	HOMO → LUMO	0.7046
	S0→S2	2.1789 eV 569.01 nm	0.3843	HOMO -1 → LUMO	0.7055
	S0→S3	2.8117 eV 440.96 nm	0.2808	HOMO -2 → LUMO	0.6943

[a] Only the selected low-lying excited states are presented. [b] Oscillator strength. [c] Only the main configurations are presented. [d] The CI coefficients are in absolute values.

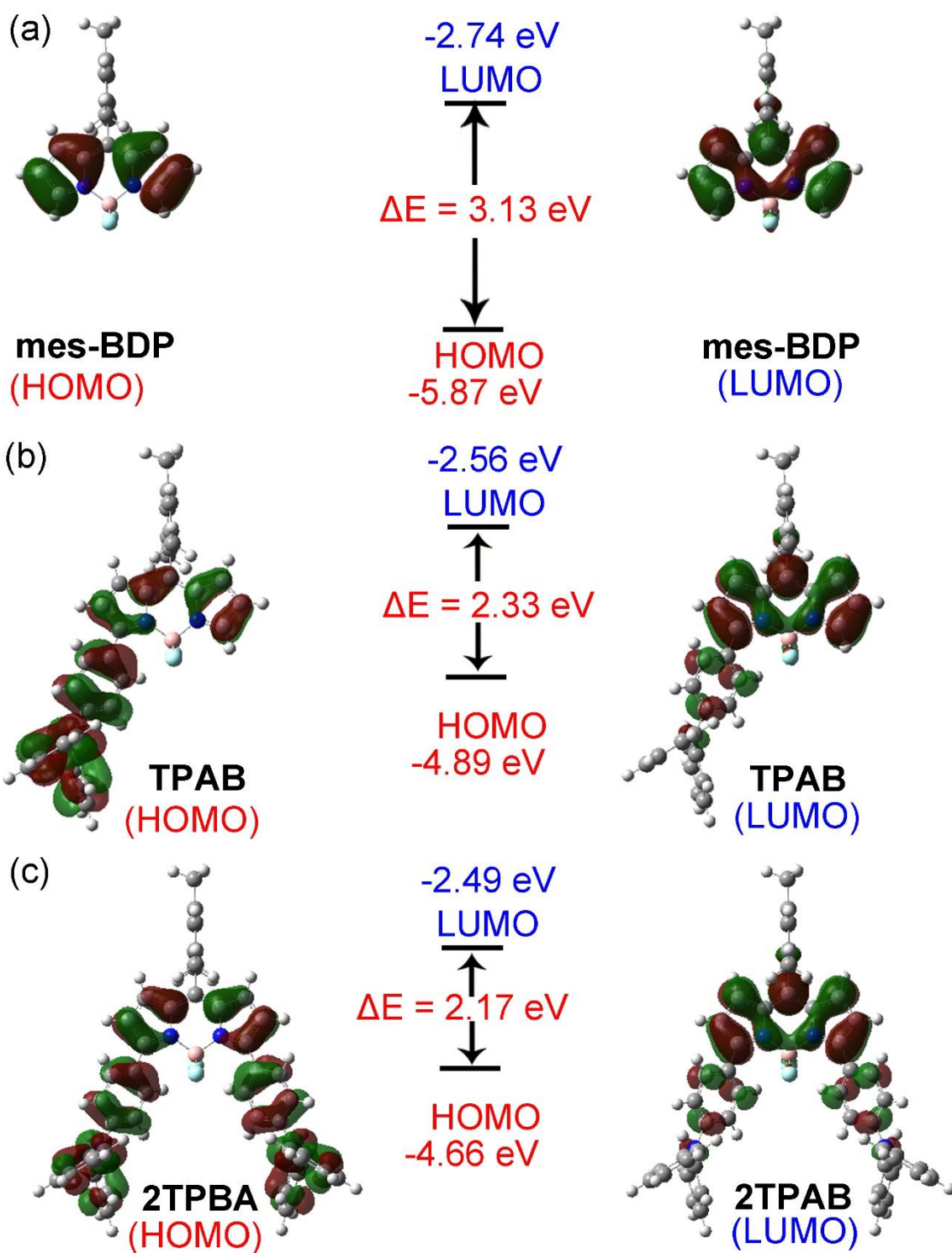


Figure S6. Molecular orbital amplitude plots of HOMO and LUMO energy levels of (a) **mes-BDP**, (b) **TPAB** and (c) **2TPAB** at B3LYP/6-31G(d) level.

DFT optimized coordinates for mes-BDP, TPAB and 2TPAB.

mes-BDP

C	0.78195000	-1.21303900	-0.02130700
N	2.17643000	-1.24284600	-0.03176200
B	3.12662000	0.00334100	0.06431400
N	2.17356800	1.24742400	-0.03074700
C	0.77916300	1.21440100	-0.02027800
C	0.07896400	-0.00013300	-0.00902500
C	0.31353900	-2.55351100	-0.05729800
C	1.43183000	-3.37577100	-0.09199900
C	2.55883500	-2.52659400	-0.07425400
C	2.55301700	2.53208700	-0.07213200
C	1.42406800	3.37868500	-0.08911200
C	0.30767900	2.55381400	-0.05507600
C	-3.50395400	-0.01088100	1.21952100
C	-4.23382800	-0.00873100	0.02761500
C	-3.52578700	-0.00845000	-1.17722100
C	-2.12784700	-0.00350100	-1.21639600
C	-1.41741200	-0.00158700	0.00200800
C	-2.10575000	-0.00596100	1.23318600
H	-0.72708200	-2.84762300	-0.06332300
H	1.45535800	-4.45617300	-0.12933300
H	1.44511900	4.45917100	-0.12550700
H	-0.73361400	2.84549900	-0.06079800
H	-4.03533100	-0.01781900	2.16909800
H	-4.07439500	-0.01345600	-2.11694600
F	4.01732400	0.00479600	-0.99138200
F	3.77929100	0.00360300	1.28336800
C	-5.74440600	0.01800900	0.04166800
H	-6.12264300	1.04888800	0.06087600
H	-6.16236700	-0.46415300	-0.84829800
H	-6.14634200	-0.49080900	0.92423400
C	-1.40962800	-0.00449200	-2.54763500
H	-0.76583600	0.87565400	-2.65922200
H	-0.76543300	-0.88447700	-2.65821300
H	-2.12523000	-0.00506900	-3.37498200
C	-1.36250900	-0.00950400	2.55051500
H	-0.71665100	-0.88990900	2.64731500
H	-0.71594700	0.86995300	2.65110700
H	-2.06213800	-0.01098100	3.39140500
H	3.60938300	-2.78525100	-0.08915800
H	3.60296800	2.79317100	-0.08682900

SCF done: -1030.383 a.u.

No imaginary Frequency.

TPAB

C	3.98590300	-1.14507000	1.25428200
N	2.77467800	-1.61259100	1.74941500
B	1.36452500	-1.33870200	1.13701100
N	1.55732500	-0.17920600	0.08580700
C	2.81591200	0.26824300	-0.33526800
C	4.01221900	-0.20843300	0.20790900
C	5.02932300	-1.72627700	2.01698400
C	4.42864300	-2.54147000	2.97242300
C	3.03859600	-2.44394800	2.77218400
C	0.61450600	0.54980300	-0.56810600
C	1.26857000	1.48471900	-1.42604200
C	2.62641200	1.30086100	-1.29291100
C	7.18507900	0.13568400	-1.83383400
C	7.80153400	1.24847200	-1.25515800
C	7.15648300	1.87526900	-0.18562800
C	5.92654900	1.42557600	0.30557500
C	5.32357800	0.30396800	-0.30110100
C	5.95543300	-0.35070600	-1.37909100
H	6.08494300	-1.54338300	1.86973700
H	4.91781600	-3.13500200	3.73262100
H	2.23250700	-2.92707400	3.30780900
H	0.76197000	2.17363500	-2.08723100
H	3.42282000	1.82759800	-1.80041100
H	7.67389500	-0.37266600	-2.66263900
H	7.62240400	2.73919500	0.28428400
F	0.48628000	-0.96422700	2.13355800
F	0.93660000	-2.49824000	0.48732700
C	-0.83789800	0.42157500	-0.44360500
C	-1.63443100	1.57081800	-0.62470100
C	-1.50028100	-0.79810300	-0.20323100
C	-3.01835900	1.51592300	-0.55803400
H	-1.15792600	2.53011800	-0.80369000
C	-2.88481700	-0.85804000	-0.13485300
H	-0.92531500	-1.70576000	-0.07479300
C	-3.67240100	0.29496600	-0.30781700
H	-3.60192900	2.41930000	-0.69914400
H	-3.36709200	-1.81028600	0.05803700
N	-5.08080000	0.23166100	-0.23503700
C	-5.82424000	1.31636000	0.31383100
C	-5.41307600	1.93136200	1.50677800
C	-6.98512800	1.77510600	-0.32745800
C	-6.14533100	2.99206200	2.03699000
H	-4.52180900	1.57284400	2.01209500
C	-7.72071800	2.82482700	0.21982100
H	-7.30452900	1.30408300	-1.25176100

C	-7.30414500	3.44275200	1.40083300
H	-5.81449100	3.45746200	2.96172000
H	-8.61764500	3.16869800	-0.28864500
H	-7.87639600	4.26478800	1.82131400
C	-5.77869700	-0.91982800	-0.70175400
C	-6.82132800	-1.47195900	0.05793000
C	-5.44204800	-1.50842500	-1.93065400
C	-7.51489700	-2.58712900	-0.40872800
H	-7.08155700	-1.02303600	1.01124800
C	-6.12923000	-2.63423000	-2.38069400
H	-4.64170800	-1.08012500	-2.52580000
C	-7.17142600	-3.17783400	-1.62655300
H	-8.31931100	-3.00362900	0.19179400
H	-5.85577600	-3.07926100	-3.33375600
H	-7.70923100	-4.05143100	-1.98369100
C	9.11522600	1.77302200	-1.78632200
H	8.95504700	2.50978800	-2.58494900
H	9.69656800	2.26766300	-1.00099800
H	9.72788400	0.96831400	-2.20654000
C	5.27153800	2.14011200	1.46675900
H	4.28415000	2.53071400	1.19447000
H	5.12211800	1.46904000	2.32032000
H	5.88577500	2.98110500	1.80192100
C	5.33081400	-1.56018500	-2.03838100
H	5.15865400	-2.36789500	-1.31772300
H	4.35756100	-1.31985100	-2.48194000
H	5.97641700	-1.94736800	-2.83220700

SCF done: -17778.893 a.u.

No imaginary Frequency.

2TPAB

C	4.02626900	-1.21718400	-0.11967600
N	2.63244000	-1.27029000	-0.14964400
B	1.72421700	-0.00144100	-0.33246700
N	2.63433900	1.26602200	-0.14944700
C	4.02808100	1.21082500	-0.11941400
C	4.72391900	-0.00370400	-0.12345700
C	4.52600100	-2.53717100	0.01548600
C	3.43203900	-3.37534400	0.08770500
C	2.25988500	-2.57526300	-0.02519900
C	2.26373000	2.57153300	-0.02479800
C	3.43706500	3.36983600	0.08833000
C	4.52977000	2.53002600	0.01601600
C	8.34754200	-0.01224800	-1.23304100
C	9.03970500	-0.01048700	-0.01893400

C	8.29384200	-0.01124500	1.16274700
C	6.89505900	-0.00688200	1.15727200
C	6.22108400	-0.00455600	-0.08192600
C	6.95029000	-0.00794000	-1.28955900
H	5.57327500	-2.80304400	0.05718600
H	3.43592800	-4.45318800	0.17102500
H	3.44255200	4.44766000	0.17183100
H	5.57743600	2.79428300	0.05781300
H	8.90853000	-0.01839200	-2.16558500
H	8.81273800	-0.01661200	2.11935000
F	0.70353500	-0.00073100	0.59301900
F	1.22988300	-0.00098000	-1.65061400
C	0.89920700	3.10551700	-0.01041000
C	0.63086200	4.24465500	0.77497900
C	-0.15643200	2.58483100	-0.78298400
C	-0.62593300	4.83176500	0.80168100
H	1.41995700	4.66812400	1.38939700
C	-1.41658900	3.16625100	-0.75677600
H	0.01446500	1.72048500	-1.41088900
C	-1.67788700	4.29818100	0.03562500
H	-0.80078400	5.70660700	1.41894200
H	-2.21322400	2.73940700	-1.35691300
N	-2.96337100	4.88711800	0.06277000
C	-3.47813800	5.43155500	1.27369200
C	-3.33930000	4.73475400	2.48461900
C	-4.13915300	6.66986200	1.27037100
C	-3.84260800	5.27512700	3.66651100
H	-2.83752500	3.77229800	2.49151400
C	-4.65499900	7.19356400	2.45443100
H	-4.24528300	7.21446200	0.33747100
C	-4.50650500	6.50387500	3.65962500
H	-3.72708400	4.72274800	4.59538800
H	-5.16415100	8.15364100	2.43462900
H	-4.90397700	6.91821600	4.58179000
C	-3.75978300	4.93349200	-1.11668100
C	-5.12770800	4.62369000	-1.06210600
C	-3.19121300	5.29807400	-2.34738500
C	-5.90812700	4.68547800	-2.21507700
H	-5.57123000	4.33528200	-0.11441800
C	-3.97576100	5.33935800	-3.49838300
H	-2.13555500	5.54597600	-2.39436600
C	-5.33828800	5.03847200	-3.44012100
H	-6.96563900	4.44165500	-2.15560900
H	-3.51964400	5.62254300	-4.44338900
H	-5.94810200	5.07832000	-4.33819200
C	10.55011700	0.01710300	0.01467200

H	10.92906000	1.04795500	0.00570000
H	10.94008500	-0.46357500	0.91816100
H	10.98005800	-0.49313500	-0.85389000
C	6.13694000	-0.00893300	2.46620500
H	5.48933700	0.87059300	2.55783500
H	5.48977700	-0.88899000	2.55589300
H	6.82726100	-0.00963800	3.31502300
C	6.24892300	-0.01113100	-2.62961400
H	5.60603200	-0.89130500	-2.74590900
H	5.60494600	0.86783000	-2.74898700
H	6.97437200	-0.01206500	-3.44858700
C	0.89456600	-3.10719300	-0.01075600
C	-0.16038400	-2.58475100	-0.78308700
C	0.62459100	-4.24606300	0.77446500
C	-1.42143300	-3.16422800	-0.75678500
H	0.01175900	-1.72056800	-1.41087500
C	-0.63310600	-4.83123100	0.80126500
H	1.41312900	-4.67086400	1.38867800
C	-1.68436000	-4.29587800	0.03548000
H	-2.21750000	-2.73605600	-1.35672800
H	-0.80921000	-5.70591300	1.41839700
N	-2.97075700	-4.88280600	0.06276300
C	-3.48615900	-5.42664100	1.27368600
C	-4.14914400	-6.66389500	1.27026300
C	-3.34599300	-4.73028200	2.48471400
C	-4.66560700	-7.18699000	2.45432200
H	-4.25631000	-7.20815800	0.33728400
C	-3.84994600	-5.27006700	3.66659900
H	-2.84268500	-3.76862800	2.49169500
C	-4.51579800	-6.49775600	3.65961400
H	-5.17628800	-8.14625300	2.43443900
H	-3.73337200	-4.71804100	4.59555500
H	-4.91376000	-6.91163100	4.58177700
C	-3.76748000	-4.92769100	-1.11653600
C	-5.13488800	-4.61567400	-1.06163500
C	-3.19974800	-5.29299400	-2.34741300
C	-5.91563800	-4.67600700	-2.21445900
H	-5.57774800	-4.32669800	-0.11381000
C	-3.98459300	-5.33281900	-3.49825900
H	-2.14450300	-5.54260300	-2.39464400
C	-5.34661800	-5.02973000	-3.43967300
H	-6.97274100	-4.43047800	-2.15473900
H	-3.52912700	-5.61659300	-4.44340300
H	-5.95667700	-5.06844600	-4.33762800

SCF done: -2527.403 a.u.

No imaginary Frequency.

3. Cytotoxicity Studies

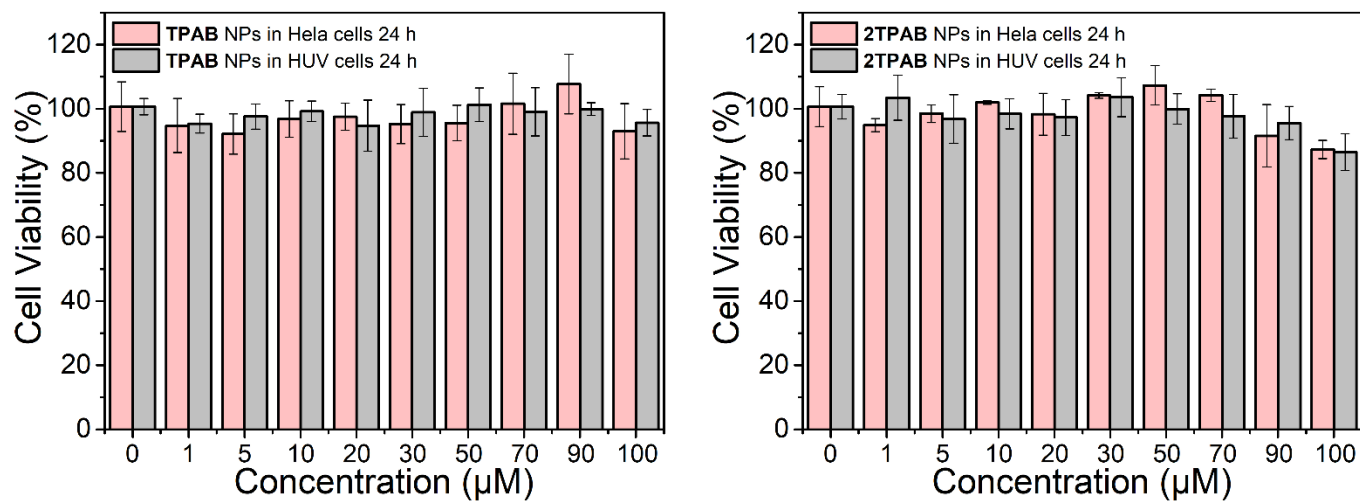


Figure S7. Cytotoxicity of HeLa (pink) or HUV-EC (gray) cells treated with different concentrations of **TPAB** (right) or **2TPAB** (left) NPs for 24 h.

4. Cellular Fluorescence Imaging

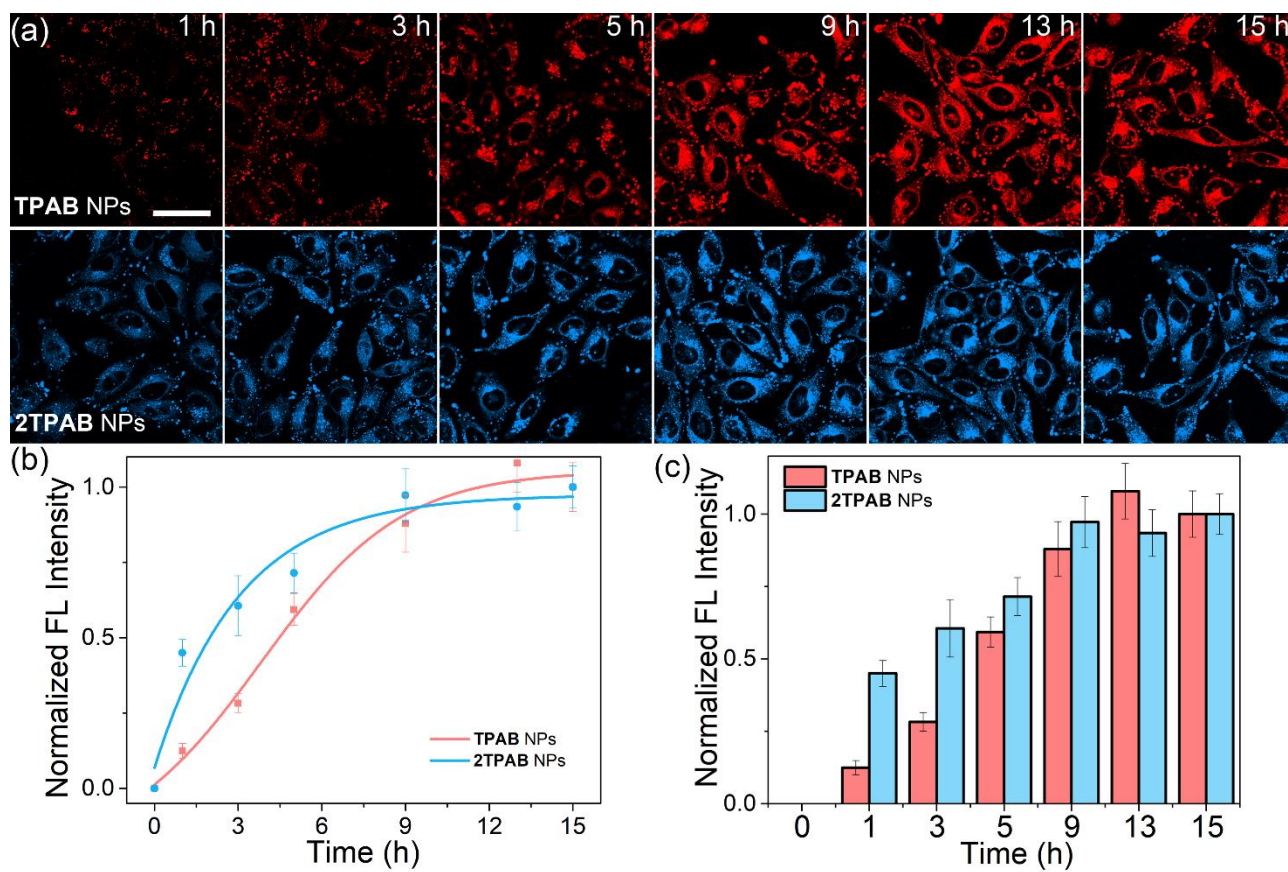


Figure S8. (a) Fluorescence microscopy images of time-dependent uptake of TPAB/2TPAB NPs at 5 μ M by HeLa cells; (b, c) Normalized fluorescence intensity quantitation was analyzed by the images. Scale bar: 50 μ m.

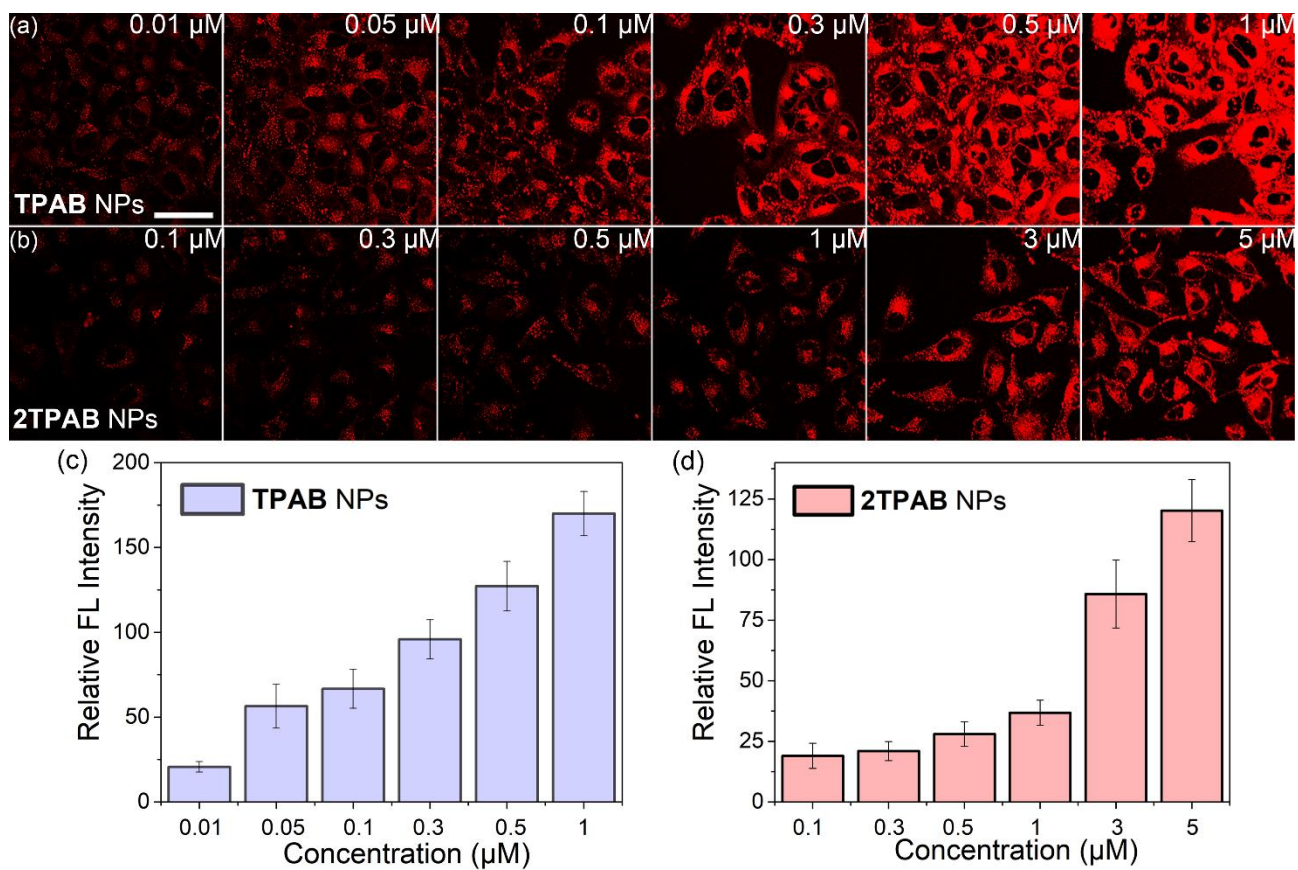


Figure S9. The concentrations of **TPAB/2TPAB** NPs for cell imaging were optimized in HeLa cells. Fluorescence microscope imaging of living HeLa cells with different concentrations of **TPAB** or **2TPAB** NPs for 3 h at 37 °C. λ_{ex} : 552 nm for **TPAB** NPs; λ_{ex} : 638 nm for **2TPAB** NPs. Scale bar: 50 μm .

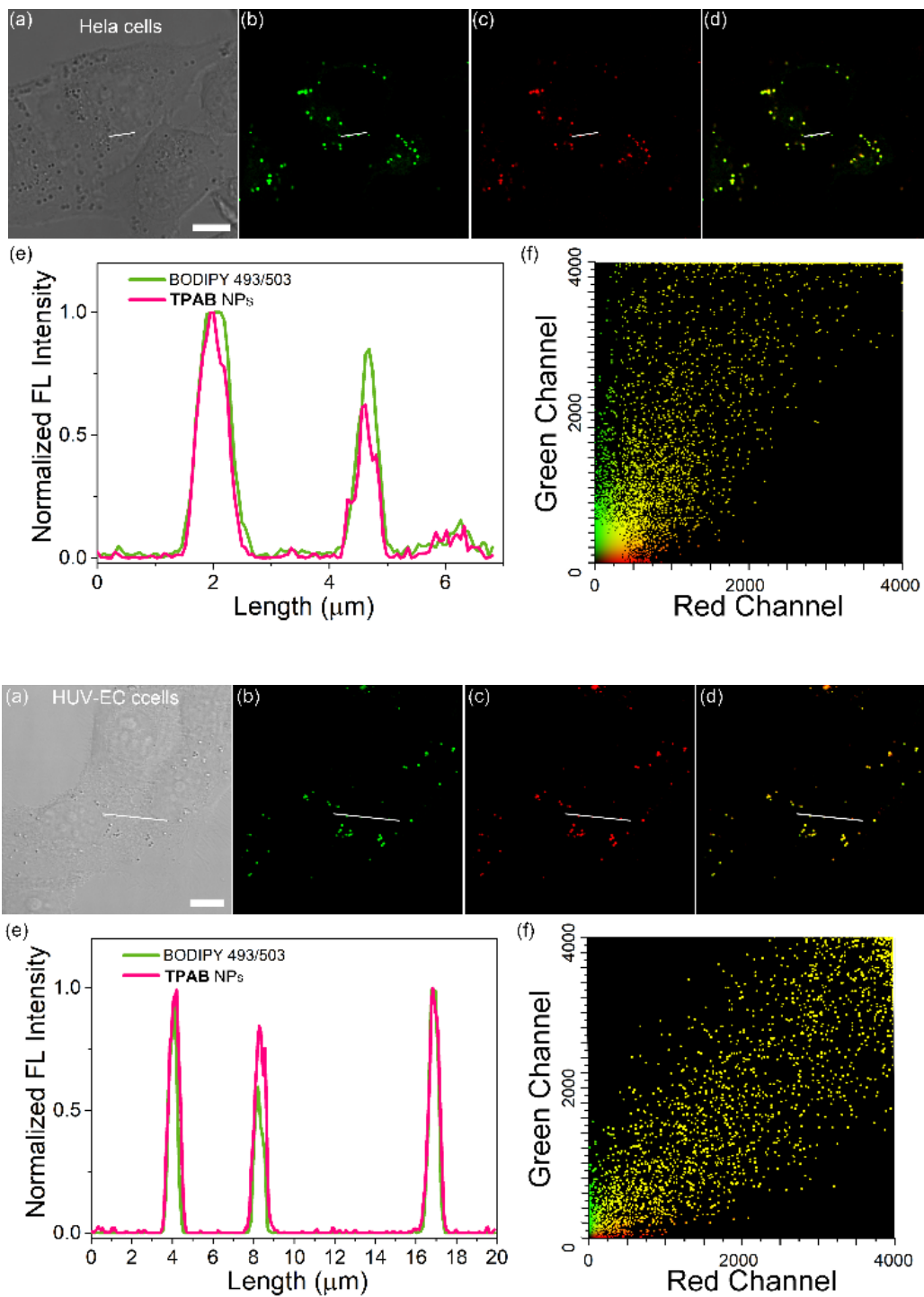


Figure S10. LD co-localization studies of **TPAB** NPs ($0.1 \mu\text{M}$) in HeLa (top) or HUV-EC (bottom) cells. (a) Bright field. (b) BODIPY 493/503 ($5 \mu\text{M}$, lipid droplets commercial dye) fluorescence, $\lambda_{\text{ex}} = 488 \text{ nm}$. (c) **TPAB** NPs fluorescence, $\lambda_{\text{ex}} = 552 \text{ nm}$. (d) Merged images of part b and c. (e) Intensity profiles within the regions of interests of **TPAB** NPs and BODIPY 493/503 across HeLa or HUV-EC cells, Pearson's correlation $R_r = 0.98$ (HeLa)/ 0.95 (HUV-EC). (f) Correlation scatter diagram of BODIPY 493/503 and **TPAB** NPs intensities, Pearson's correlation $R_r = 0.90$ (HeLa)/ 0.95 (HUV-EC); overlap coefficient $R = 0.91$ (HeLa)/ 0.95 (HUV-EC). Scale bars = $10 \mu\text{m}$.

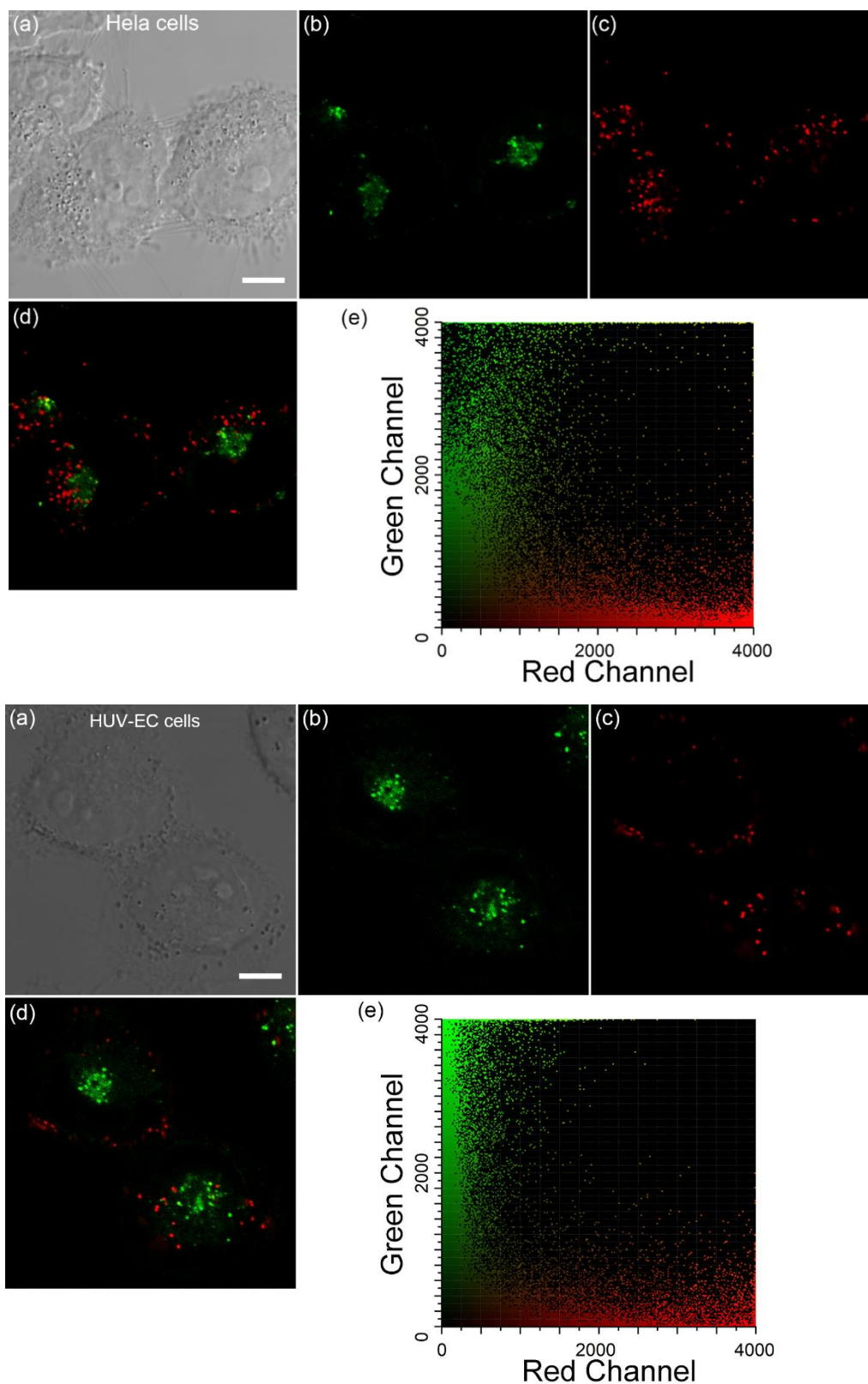


Figure S11. Lysosome co-localization studies of **TPAB** NPs (0.1 μM) in HeLa (top) or HUV-EC (bottom) cells. (a) Bright field. (b) LysoTracker Green DND-26 (1 μM , lysosome commercial dye) fluorescence, $\lambda_{\text{ex}} = 488$ nm. (c) **TPAB** NPs fluorescence, $\lambda_{\text{ex}} = 552$ nm. (d) Merged images of parts b and c. (e) Correlation scatter diagram of LysoTracker Green DND-26 and **TPAB** NPs intensities, Pearson's correlation $R_r = 0.24$ (HeLa)/0.13 (HUV-EC); overlap coefficient $R = 0.26$ (HeLa)/0.17 (HUV-EC). Scale bars = 10 μm .

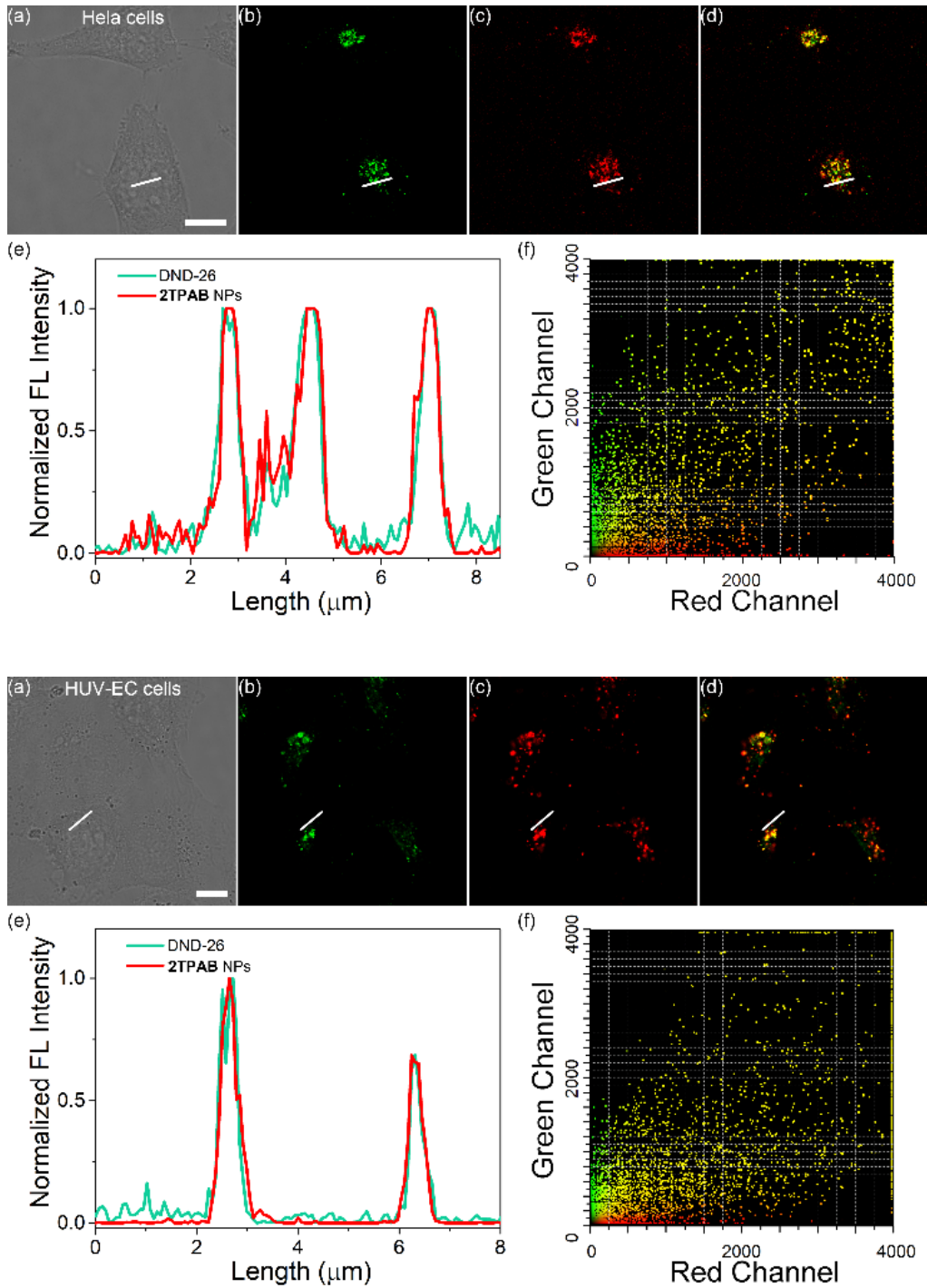


Figure S12. Lysosome co-localization studies of **2TPAB** NPs (5 μM) in HeLa (top) or HUV-EC (bottom) cells. (a) Bright field. (b) LysoTracker Green DND-26 (1 μM , lysosome commercial dye) fluorescence, $\lambda_{\text{ex}} = 488$ nm. (c) **2TPAB** NPs fluorescence, $\lambda_{\text{ex}} = 638$ nm. (d) Merged images of parts b and c. (e) Intensity profiles within the regions of interests of **2TPAB** NPs and Lyso-tracker Green DND-26 across HeLa or HUV-EC cells, Pearson's correlation $R_r = 0.95$ (HeLa)/ 0.95 (HUV-EC). (f) Correlation scatter diagram of Lyso-tracker Green DND-26 and **2TPAB** NPs intensities, Pearson's correlation $R_r = 0.81$ (HeLa)/ 0.84 (HUV-EC); overlap coefficient $R = 0.83$ (HeLa)/ 0.85 (HUV-EC). Scale bars = 10 μm .

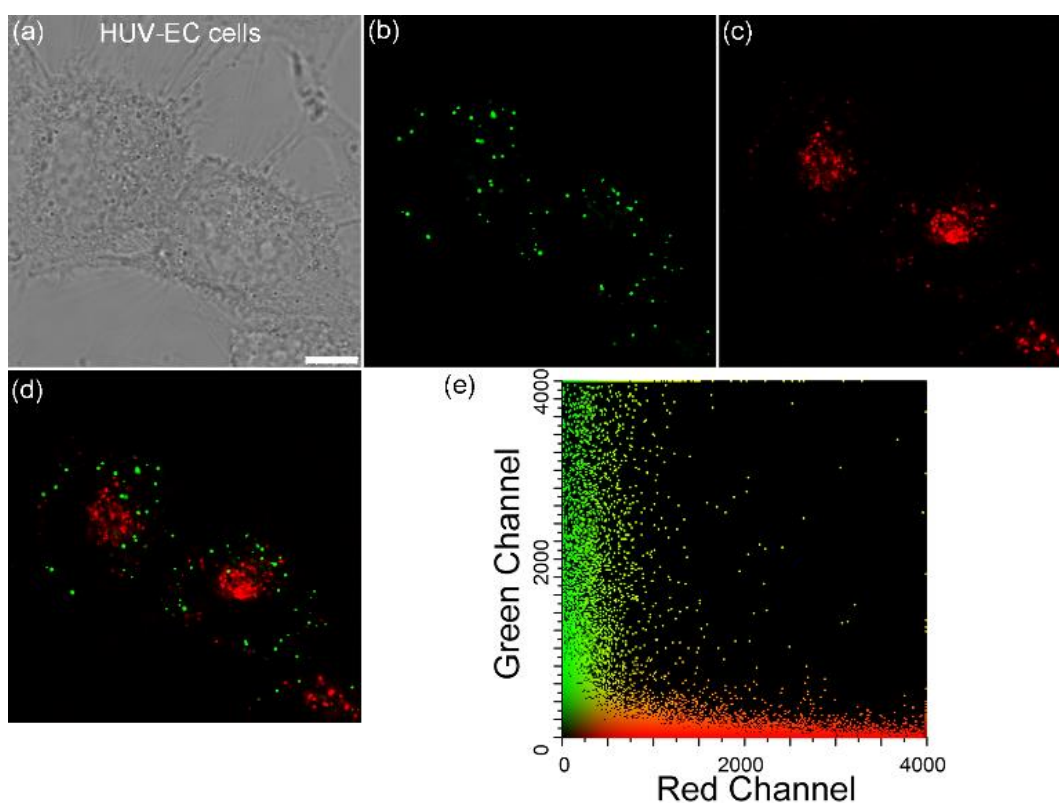
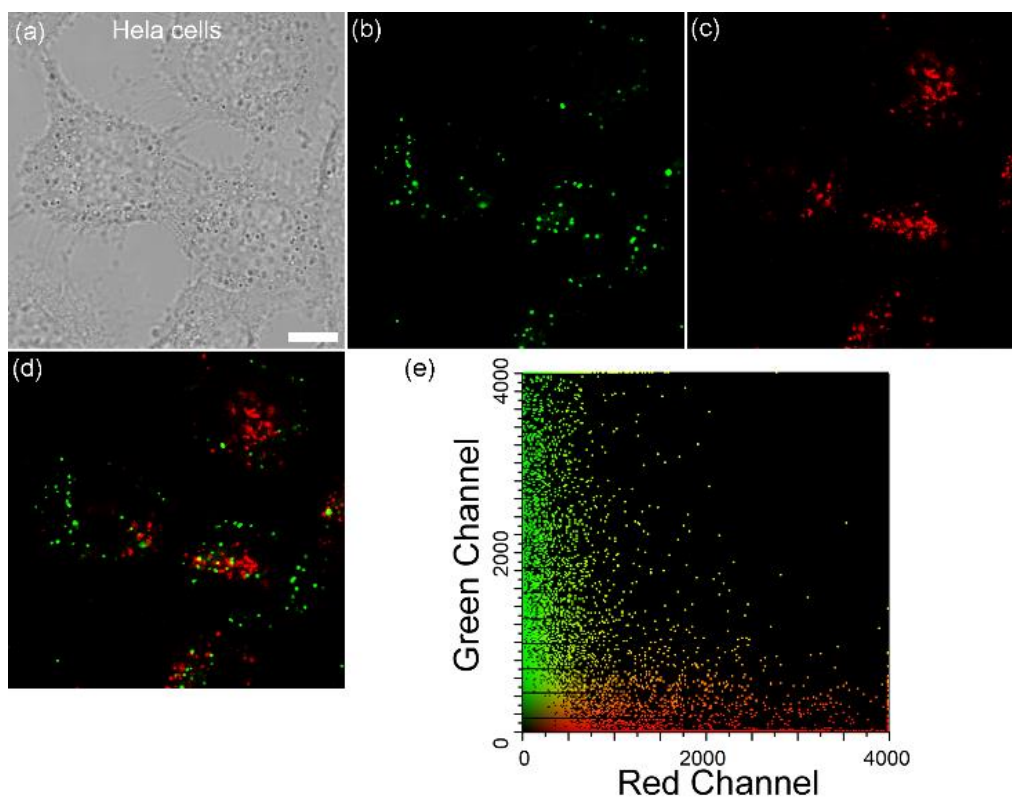


Figure S13. LDs co-localization studies of **2TPAB** NPs (5 μ M) in HeLa (top) or HUV-EC (bottom) cells. (a) Bright field. (b) BODIPY 493/503 (5 μ M, LDs commercial dye) fluorescence, $\lambda_{\text{ex}} = 488$ nm. (c) **2TPAB** NPs fluorescence, $\lambda_{\text{ex}} = 638$ nm. (d) Merged images of parts b and c. (e) Correlation scatter diagram of BODIPY 493/503 and **2TPAB** NPs intensities, Pearson's correlation $R_r = 0.15$ (HeLa)/ 0.09 (HUV-EC); overlap coefficient $R = 0.22$ (HeLa)/ 0.11 (HUV-EC). Scale bars = 10 μ m.

The preparation of TPAB and 2TPAB aggregates

TPAB aggregates: TPAB aggregates were prepared by a nanoprecipitation method. A certain amount of TPAB (15 μL , 2 mM) in high-purity solvent DMSO were injected into 1640 complete medium (3 mL). The sudden solubility decreases in culture medium resulted in self-assembly of TPAB into corresponding aggregates (10 μM , 3 mL). Then the solution was diluted to 0.1 μM for further co-localization studies.

The same methods were used to give 2TPAB aggregates.

The preparation of BODIPY 493/503 NPs and LysoTracker DND-99 NPs

BODIPY 493/503 NPs: Chloroform solution of BODIPY 493/503 (44 μL , 566 μM) and chloroform solution of F-127 (30 μL , 7.1 mg mL^{-1}) were added to a flask contained 1 mL chloroform. The obtained mixture was then dried under vacuum in a rotary evaporator to remove the chloroform completely. After that, deionized water or culture medium (5 mL) was added, and the flask was placed under sonication for several minutes to give the aqueous dispersion of BODIPY 493/503 NPs (5 μM , 5 mL).

The same methods were used to give LysoTracker DND-99 NPs.

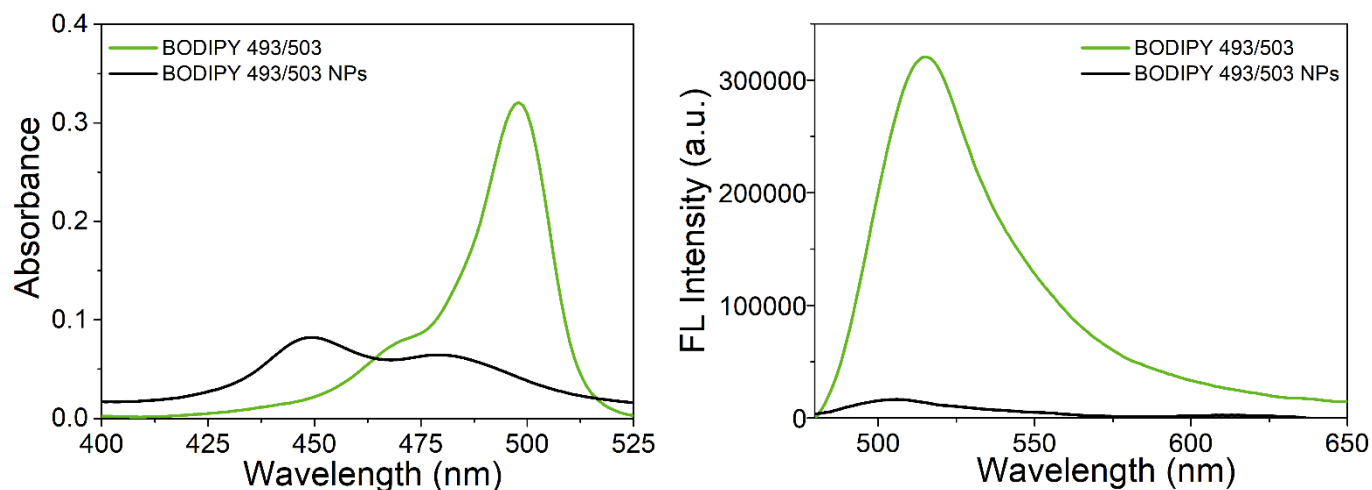


Figure S14. Absorption (left) and fluorescence (right) spectra of BODIPY 493/503 (in chloroform, green line) or BODIPY 493/503 NPs wrapped with F-127 (in deionized water, black line) at 5 μM , excited at 480 nm.

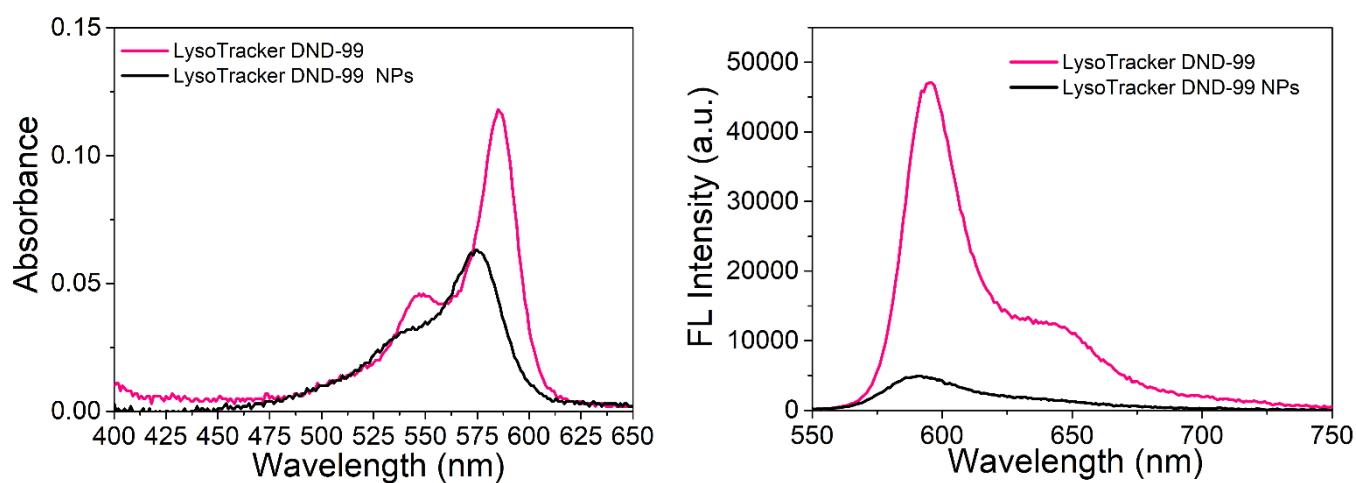


Figure S15. Absorption (left) and fluorescence (right) spectra of LysoTracker DND-99 (in chloroform, pink line) or LysoTracker DND-99 NPs wrapped with F-127 (in deionized water, black line) at 2 μM , excited at 520 nm.

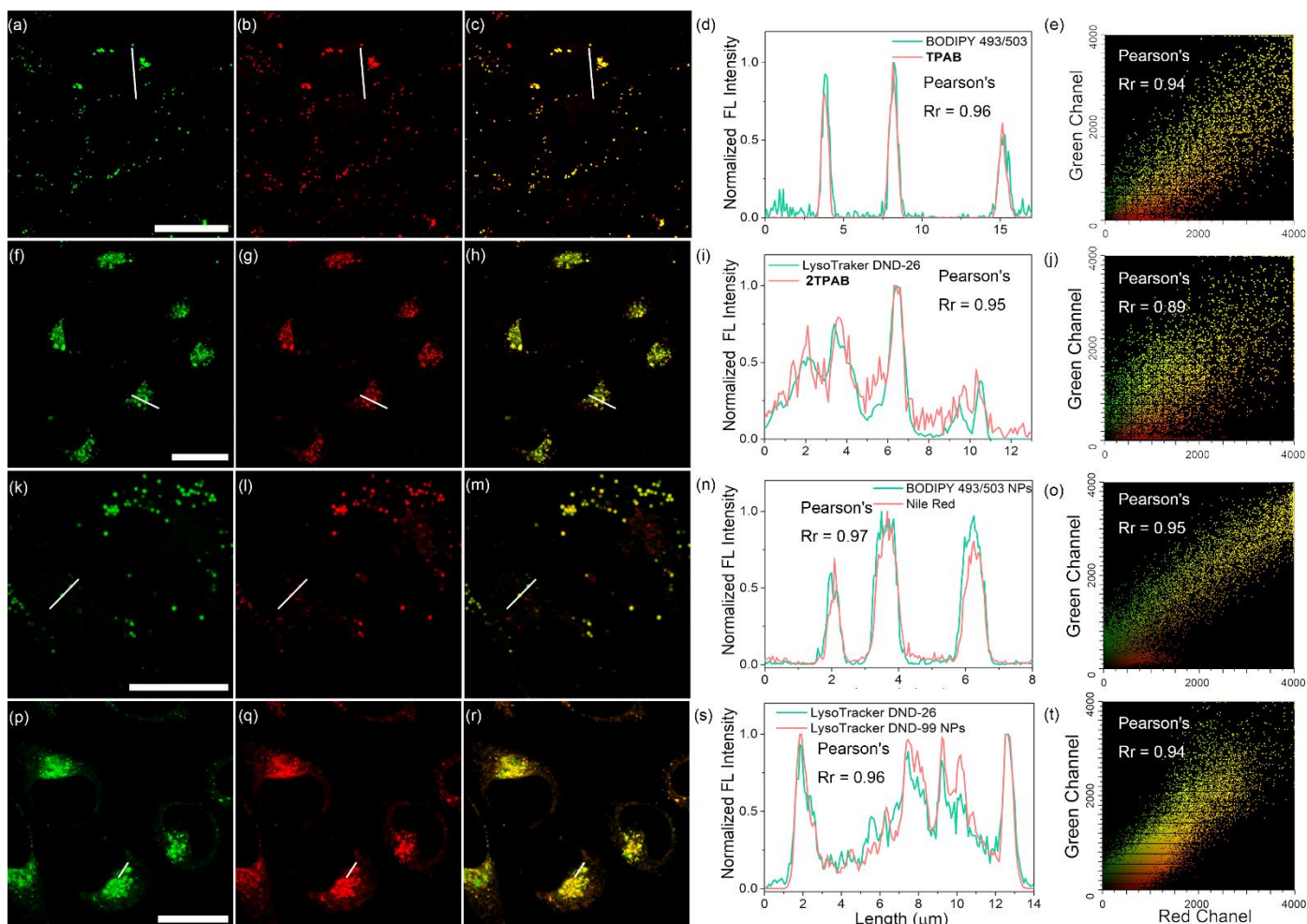


Figure S16. LDs or lysosomes co-localization studies of **TPAB**, **2TPAB**, BODIPY 493/503 NPs or LysoTracker DND-99 NPs in HeLa cells. (a) BODIPY493/503 (0.1 μM). (b) **TPAB** aggregates (0.1 μM) were prepared by the above steps. (f) LysoTracker DND-26 (0.1 μM). (g) **2TPAB** aggregates (5 μM) were prepared by the above steps. (k) BODIPY 493/503 NPs wrapped with F-127 (5 μM) were prepared by the above steps. (l) Nile Red (0.1 μM). (p) LysoTracker DND-26 (0.1 μM). (q) LysoTracker DND-99 NPs wrapped with F-127 (2 μM) were prepared by the above steps. (c, h, m, r) Overlay images of green channel and red channel. (d, i, n, s) Intensity profiles within the regions of interests across HeLa cells, Pearson's correlation $R_r = 0.96/0.95/0.97/0.96$, respectively. (e, j, o, t) Correlation scatter diagram, Pearson's correlation $R_r = 0.94/0.89/0.95/0.94$; overlap coefficient $R = 0.94/0.91/0.96/0.95$, respectively. Scale bars = 25 μm .

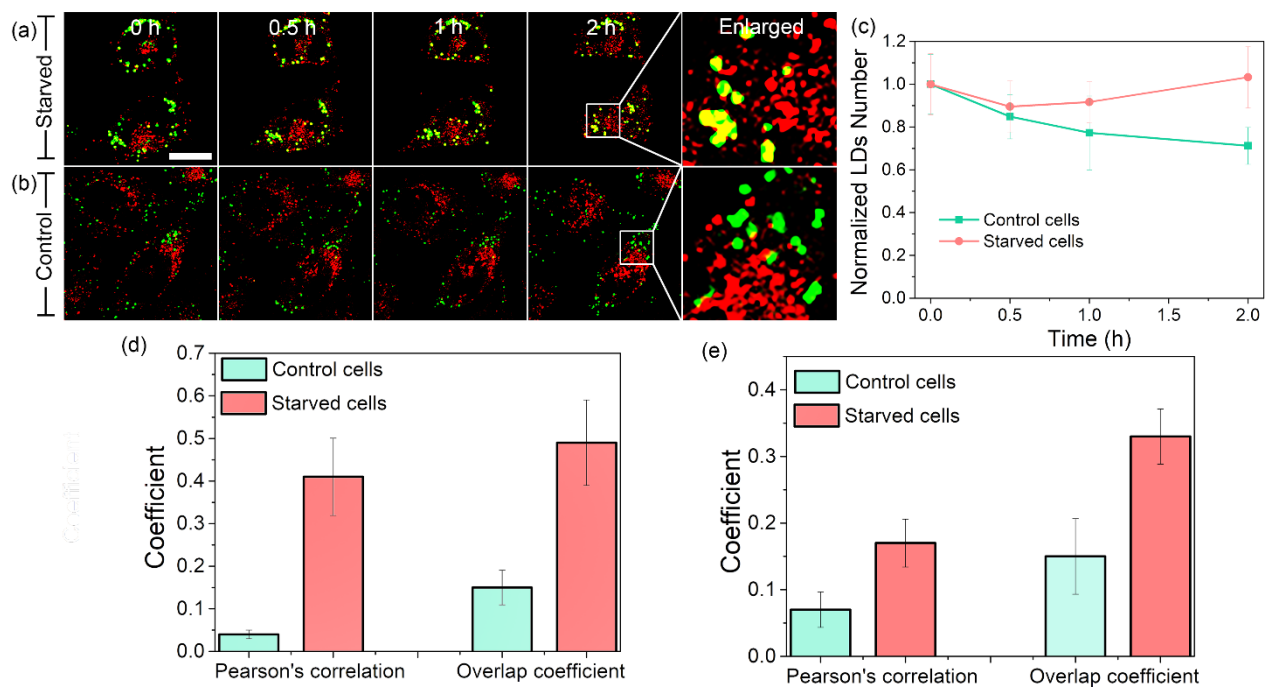


Figure S17. Monitoring lipophagy under starvation (a, starved cells) and normal (b, control cells) conditions with BODIPY 493/503 (0.1 μ M, green channel) and LysoTracker DND-99 (0.1 μ M, red channel) in living HeLa cells. Starvation conditions: the cells were incubated with LysoTracker DND-99 and BODIPY 493/503 for 1 h then treated with nutrient-free medium for 2 h and observation at room temperature. (c) Average number of LDs changes during the lipophagy process of part a and b. (d) Correlation coefficients for BODIPY 493/503 and LysoTracker DND-99 of starved and control cells from the enlarged images. Control cells: Pearson's correlation $R_r = 0.04$; overlap coefficient $R = 0.15$; Starved cells: Pearson's correlation $R_r = 0.41$; overlap coefficient $R = 0.49$. (e) Correlation coefficients for BODIPY 493/503 and 2TPAB NPs of starved and control cells from the enlarged images (Figure 6d and 6e). Control cells: Pearson's correlation $R_r = 0.07$; overlap coefficient $R = 0.15$; Starved cells: Pearson's correlation $R_r = 0.17$; overlap coefficient $R = 0.33$. Scale bar: 15 μ m.

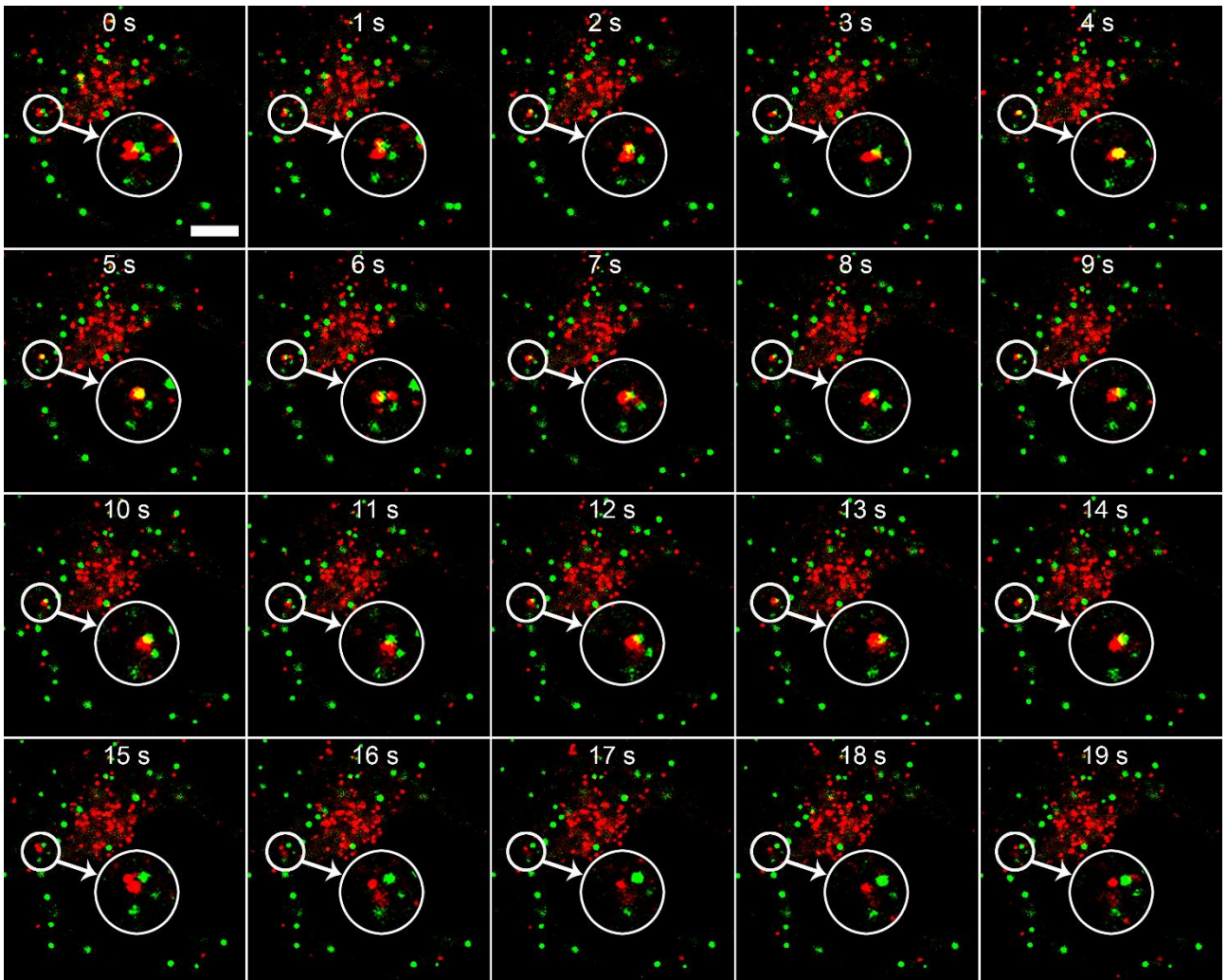


Figure S18. Monitoring the momentary contact between LD and lysosome at different times in living HeLa cells. Green channel: BODIPY 493/503 (0.1 μM); Red channel: 2TPAB NPs (5 μM).

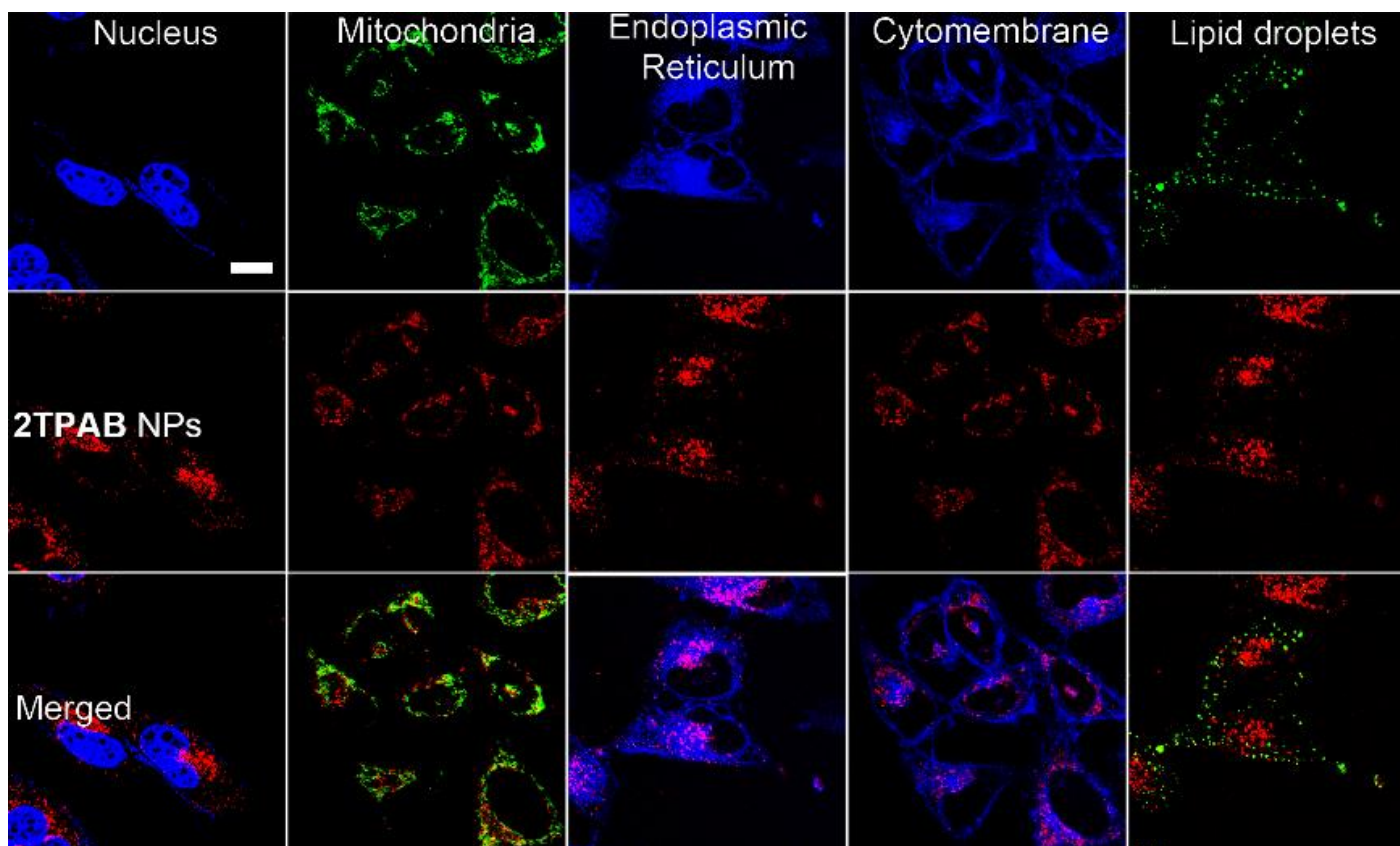


Figure S19. Multicolor images of **2TPAB** NPs with commercial organelle dyes in HeLa cells. The upper row images represent organelle dyes (nucleus: DAPI, $0.1 \mu\text{g mL}^{-1}$; mitochondria: Rhodamine 123, $10 \mu\text{M}$; endoplasmic reticulum: ER-Tracker Blue-White DPX, $0.5 \mu\text{M}$; cytoplasm: Laudan, $1 \mu\text{M}$; Lipid droplets: BODIPY 493/503, $5 \mu\text{M}$) and the middle row are **2TPAB** NPs. The bottom row images represent overlay images. Scale bar is $10 \mu\text{m}$.

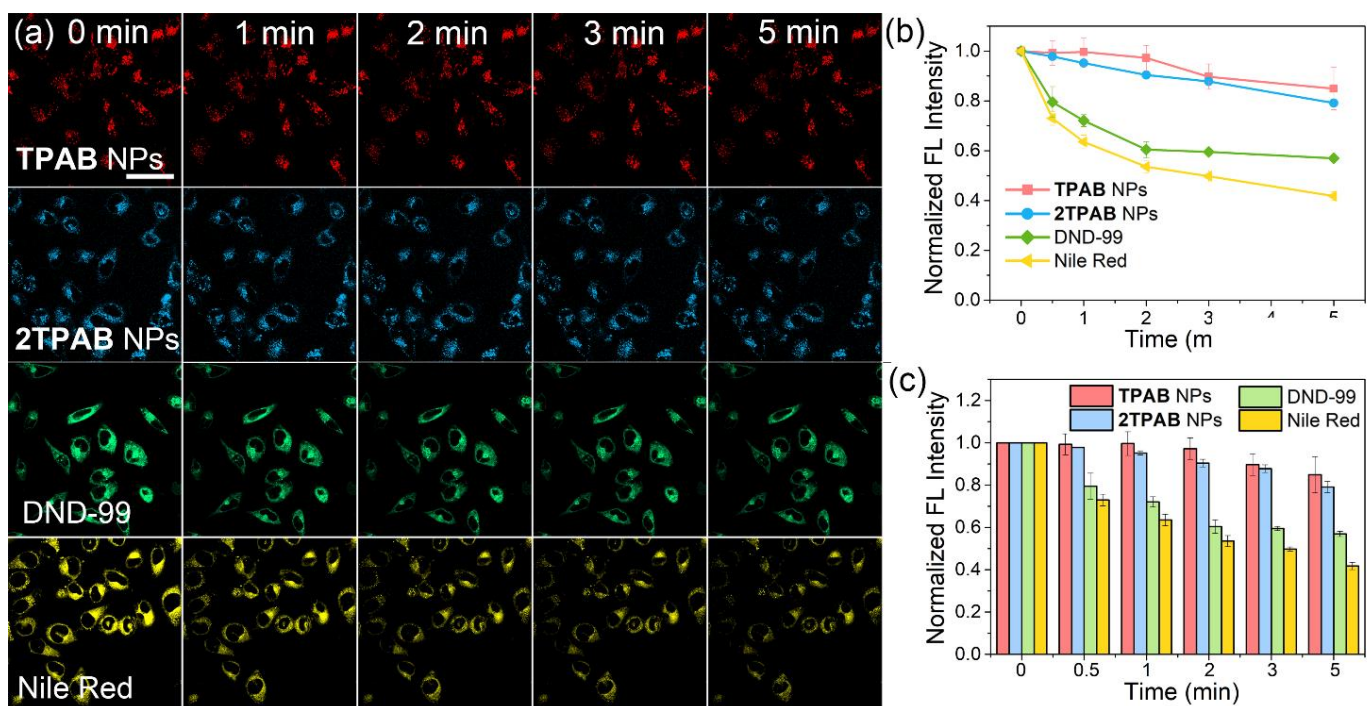


Figure S20. (a) Fluorescent images and (b, c) normalized fluorescence intensity of **TPAB** (0.1 μM) or **2TPAB** NPs (5 μM), LysoTracker DND-99 or Nile Red by continuous irradiation laser at different time with the same laser power of 30%, λ_{ex} : 552 nm. The image was scanned at different time. Scale bar: 50 μm .

The calculation of two-photon cross section and cellular imaging

The two-photon-induced fluorescent spectra of **TPAB** or **2TPAB** were determined with the same excitation wavelength (from 700 to 1000 nm, every 10 nm) using fluorescein as the reference by femtosecond two-photon excited fluorescence (TPEF) technique. The Two-photon cross section was calculated by using the below equation according to previous reports.²

$$\delta_2 = \frac{\delta_1 \Phi_1 (F_2 c_1)}{\Phi_2 (F_1 c_2)}$$

In which the subscripts 1 and 2 refer to the reference of fluorescein and our probe **TPAB/2TPAB**, respectively; F is the integration of the fluorescent spectra; Φ is the fluorescence quantum yield ($\Phi = 0.95$ for fluorescein, NaOH solution, pH = 11; $\Phi = 0.96$ for **TPAB** in *n*-hexane solution, $\Phi = 0.83$ for **2TPAB** in *n*-hexane solution); c is the concentration of fluorescein (100 μM) and our sample (100 μM); and δ_1 is the TPA cross-section of the reference of fluorescein according to previous reports.⁴

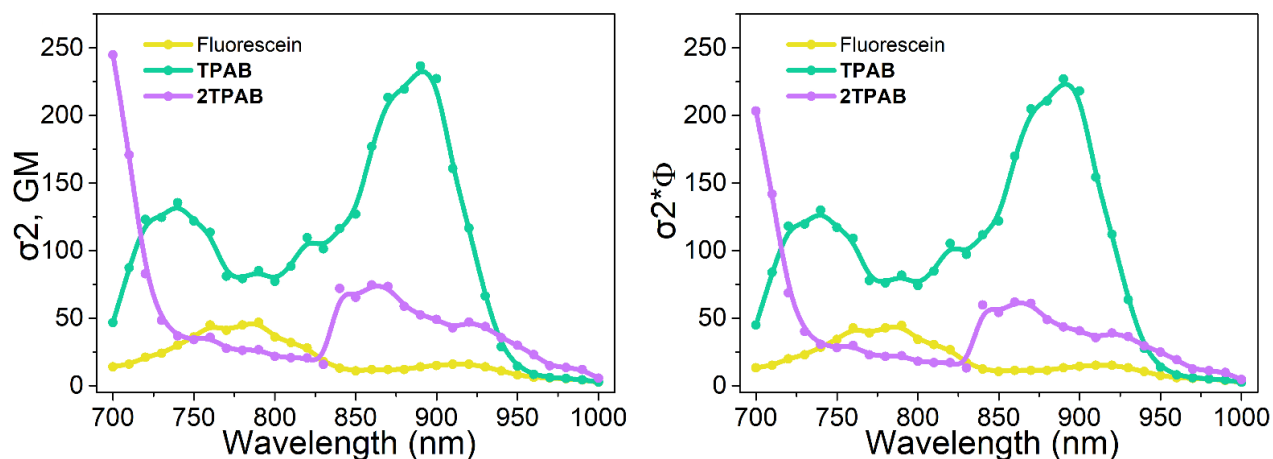


Figure S21. (a) Two-photon cross section fluorescence spectra of **TPAB/2TPAB** (100 μ M, in *n*-hexane solution) or fluorescence (100 μ M, NaOH solution, pH = 11) at different excitation wavelength by the above equation. (b) The activity Two-photon cross section fluorescence spectra of **TPAB/2TPAB** or fluorescence at different excitation wavelength.

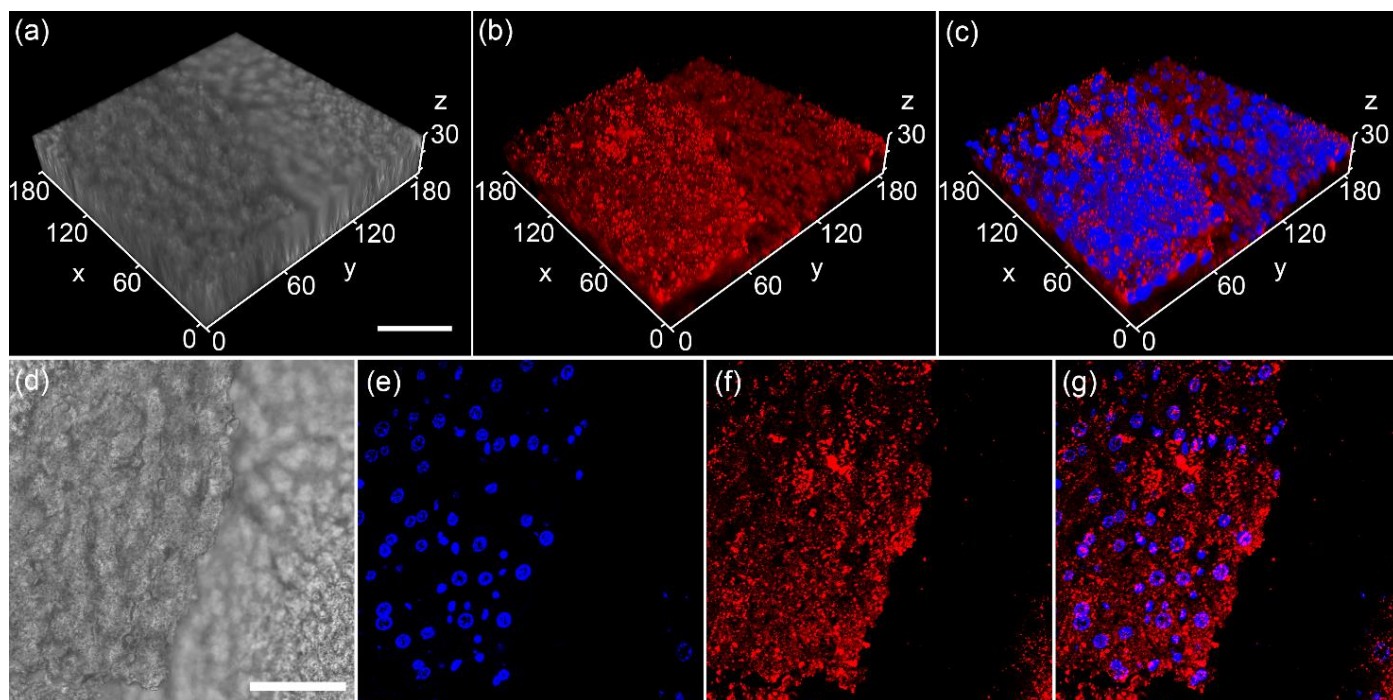
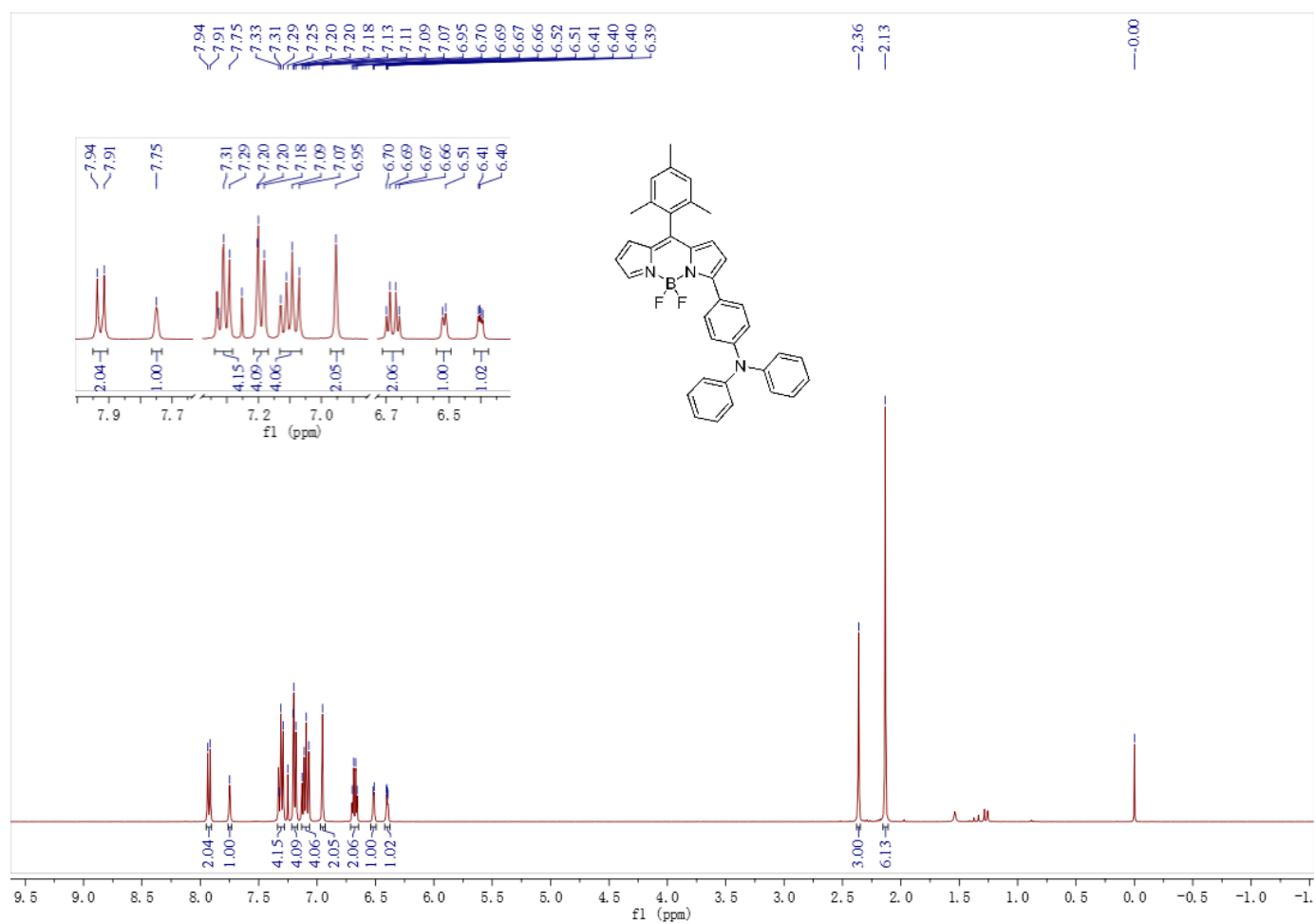
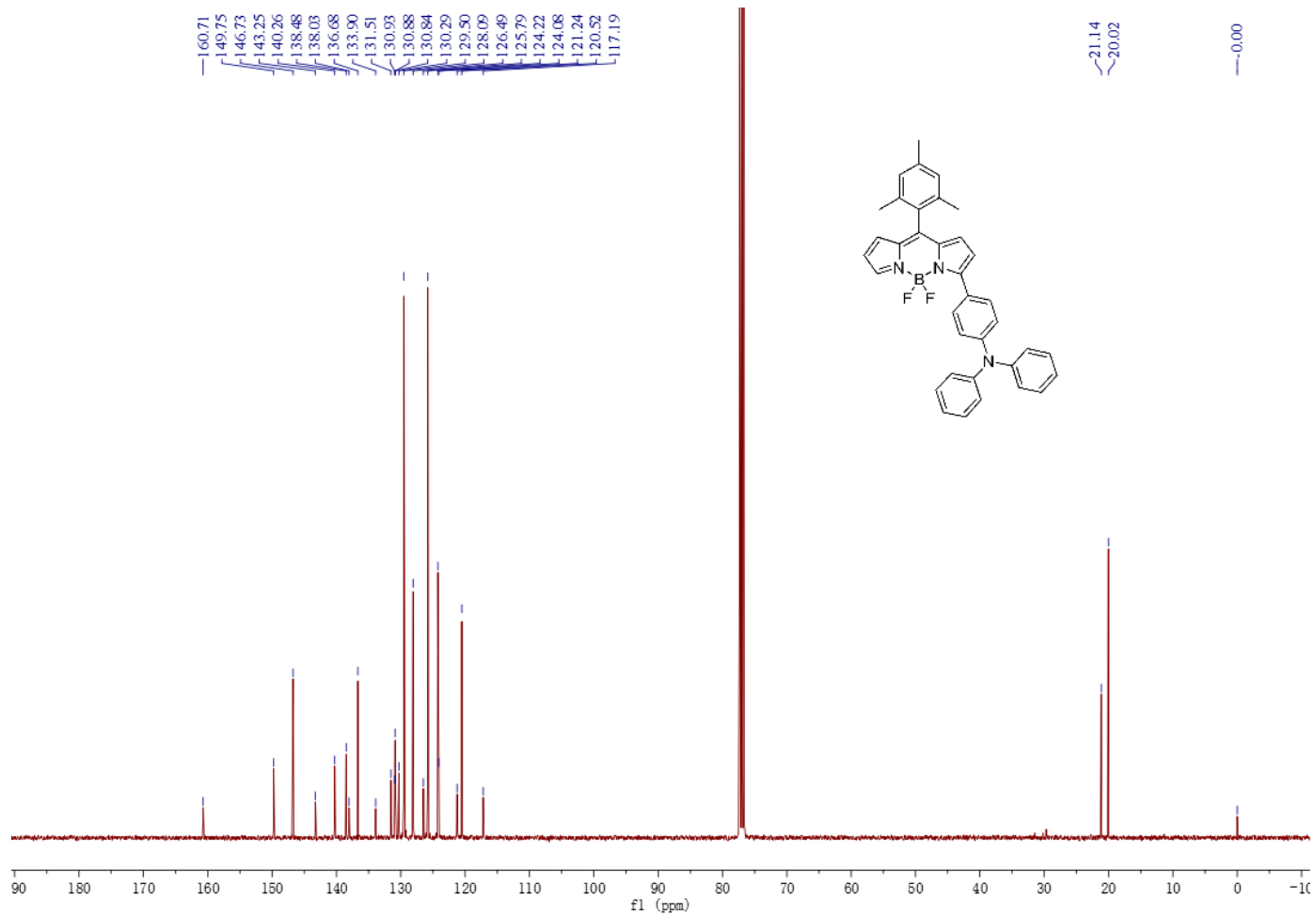


Figure 22. Ex vivo fluorescent imaging in mice's liver tissues. (a) Reconstructed 3D microscopic bright fields images. (b) Reconstructed 3D fluorescent microscopic images. Blue channel: liver tissues stained with DAPI (0.1 μ g mL⁻¹, nuclear commercial dye) fluorescence, λ_{ex} : 405 nm; Red channel: liver tissues stained with **2TPAB** NPs (10 μ M) after incubation for 5 h, λ_{ex} : 638 nm; λ_{em} : 650-800 nm. (c) Reconstructed 3D fluorescent microscopic overlay images. Scale bar: 50 μ m. (d) Bright fields of mice's liver tissues cross-sections. (e, f) Fluorescence images of the tissues stained with DAPI and **2TPAB** NPs. (g) Overlay images of e and f. Scale bar: 30 μ m.

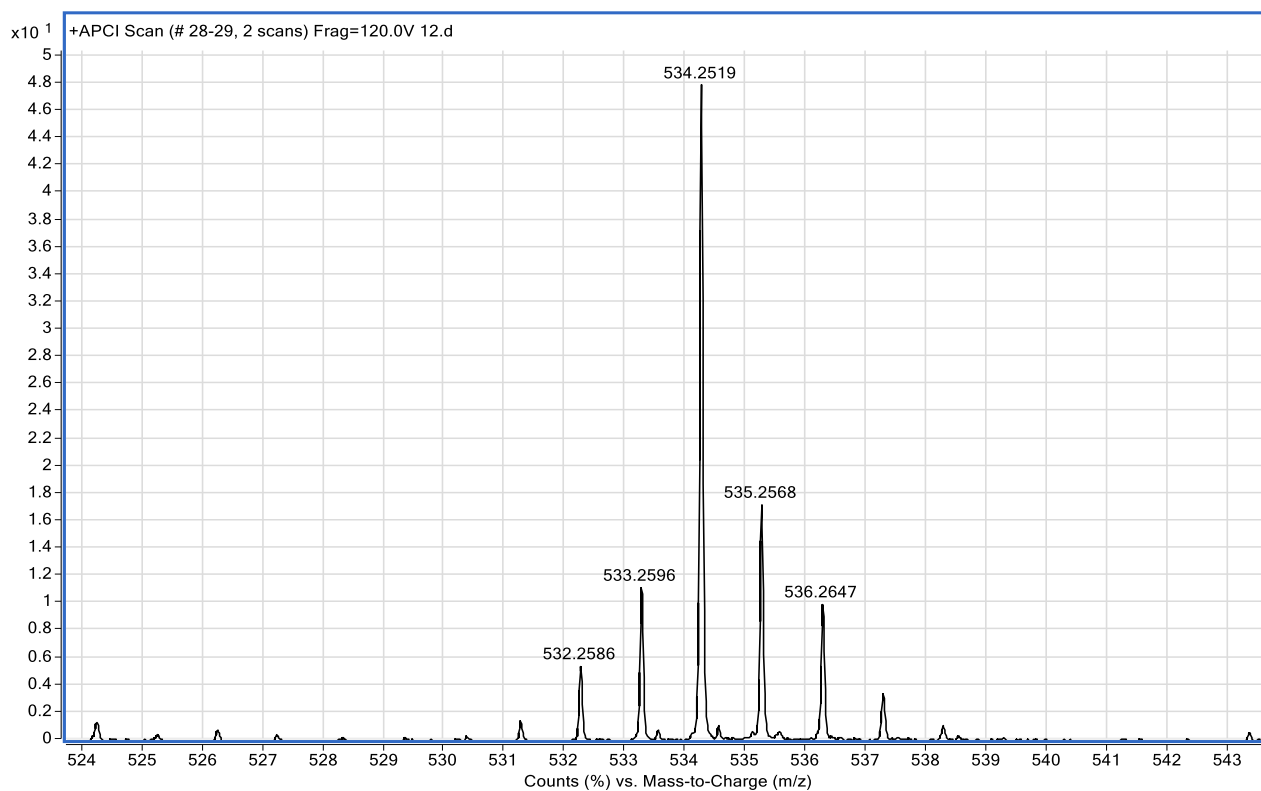
5. ^1H , ^{13}C and HRMS spectra for TPAB and 2TPAB



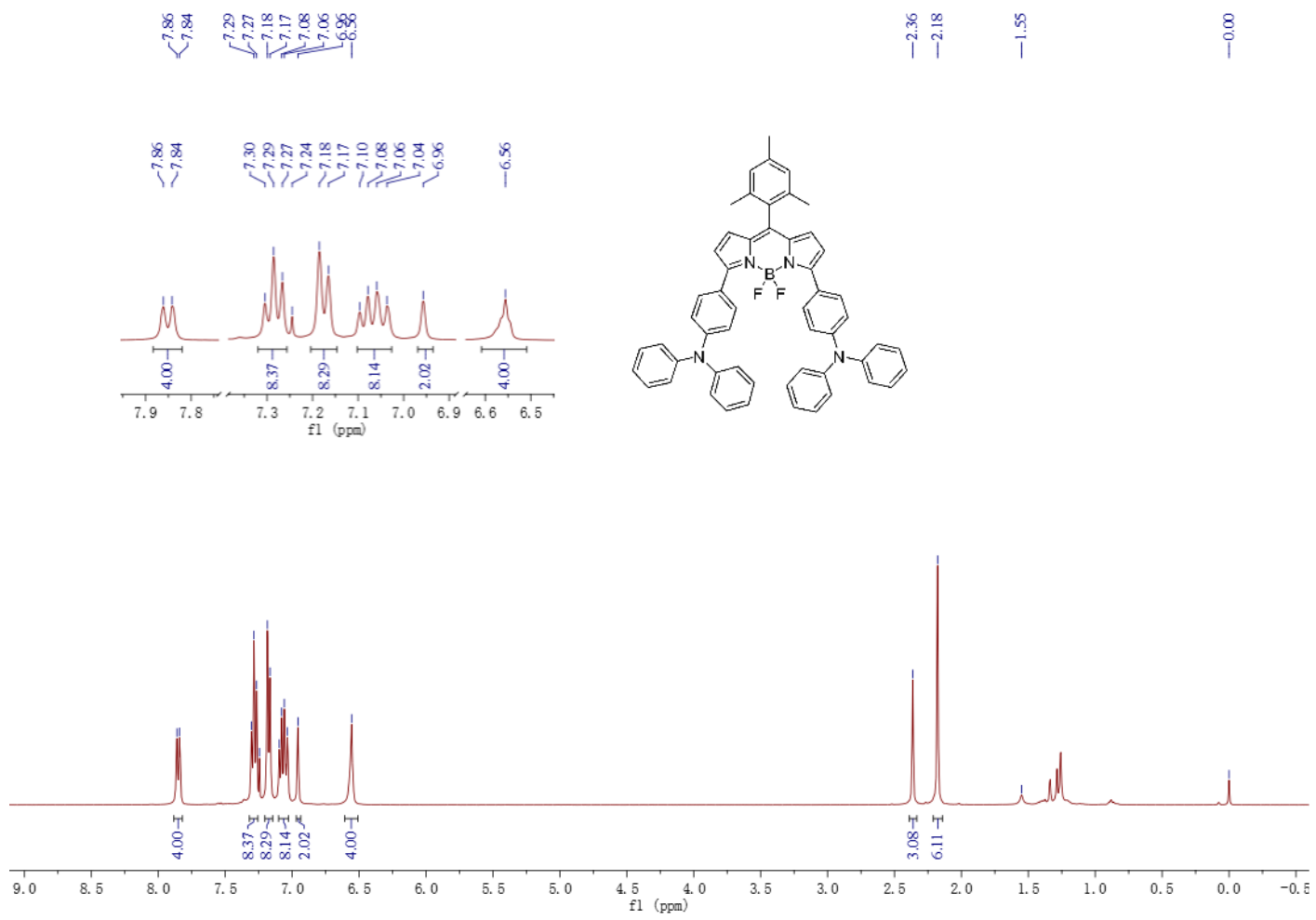
^1H NMR spectrum of TPAB in CDCl_3



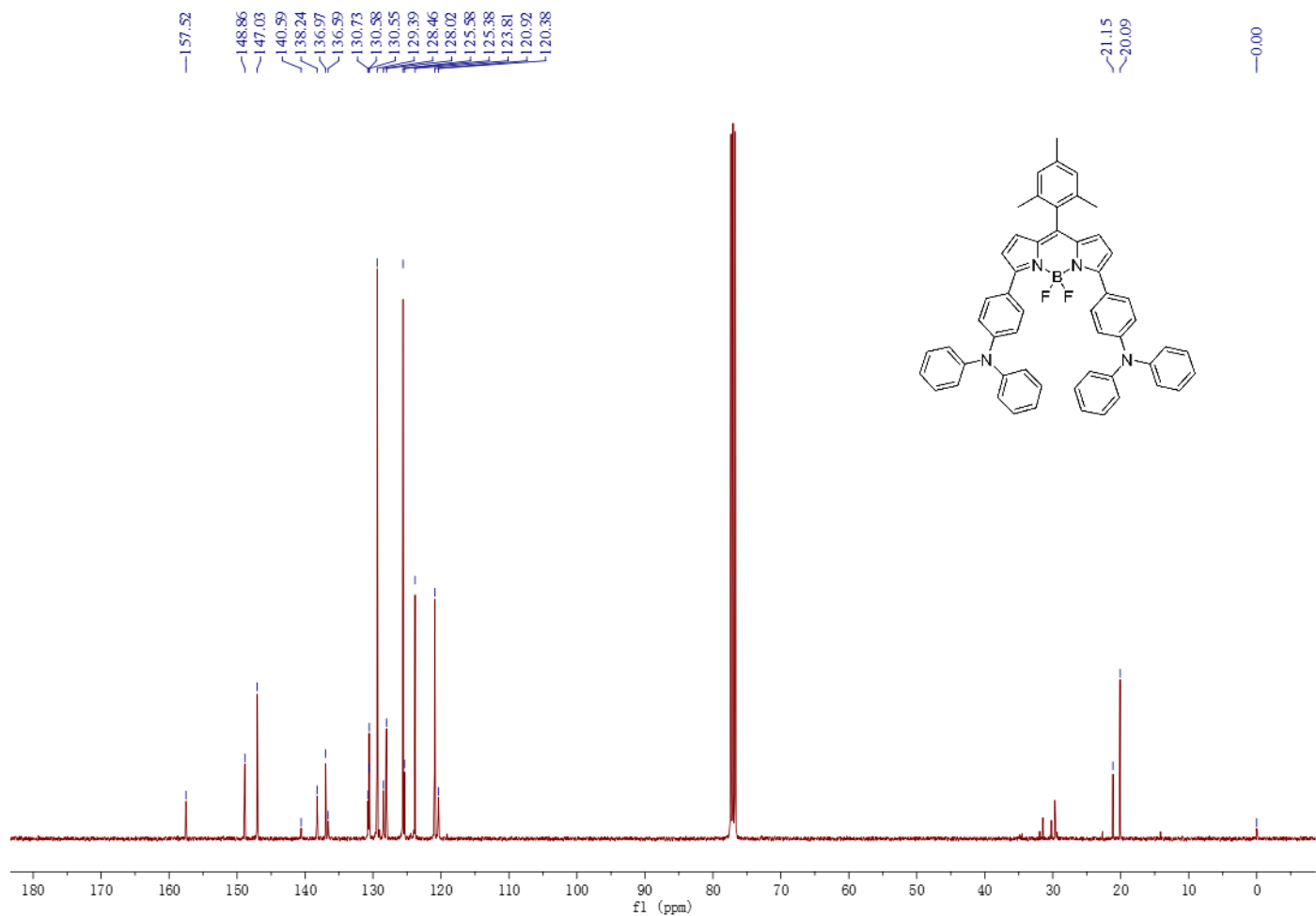
^{13}C NMR spectrum of **TPAB** in CDCl_3



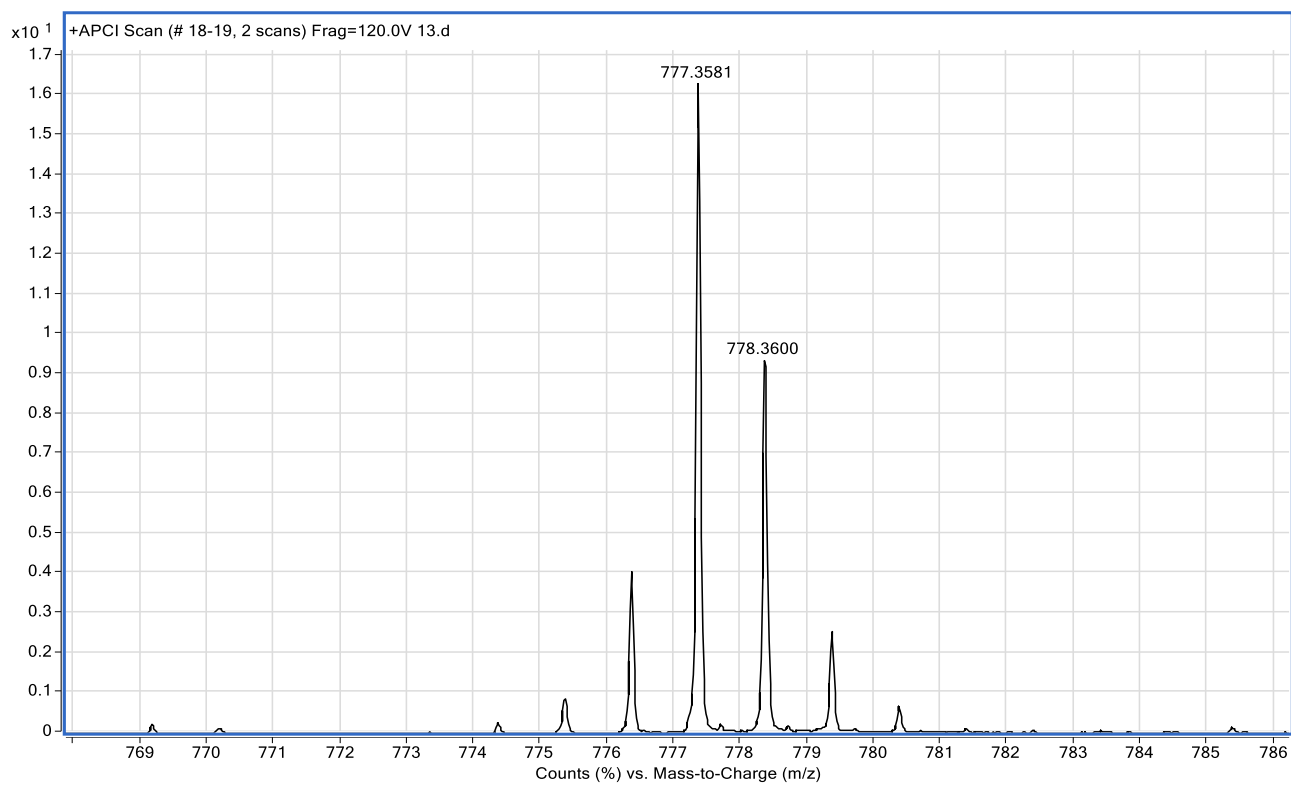
HRMS for **TPAB**



^1H NMR spectrum of **2TPAB** in CDCl_3



^{13}C NMR spectrum of **2TPAB** in CDCl_3



HRMS for **2TPAB**

7. References

- (1) J. I. Stefan, M. E. Edward, Fluorescence quantum yield of cresyl violet in methanol and water as a function of concentration, *J. Phys. Chem.* 1992, **96**, 1738.
- (2) J. Olmsted, Calorimetric determinations of absolute fluorescence quantum yields, *J. Phys. Chem.* 1979, **83**, 2581.
- (3) Gaussian 09, Revision D.01, M. J. Frisch, G. W. Trucks, H. B. Schlegel, G. E. Scuseria, M. A. Robb, J. R. Cheeseman, G. Scalmani, V. Barone, B. Mennucci, G. A. Petersson, H. Nakatsuji, M. Caricato, X. Li, H. P. Hratchian, A. F. Izmaylov, J. Bloino, G. Zheng, J. L. Sonnenberg, M. Hada, M. Ehara, K. Toyota, R. Fukuda, J. Hasegawa, M. Ishida, T. Nakajima, Y. Honda, O. Kitao, H. Nakai, T. Vreven, J. A. Montgomery, Jr., J. E. Peralta, F. Ogliaro, M. Bearpark, J. J. Heyd, E. Brothers, K. N. Kudin, V. N. Staroverov, T. Keith, R. Kobayashi, J. Normand, K. Raghavachari, A. Rendell, J. C. Burant, S. S. Iyengar, J. Tomasi, M. Cossi, N. Rega, J. M. Millam, M. Klene, J. E. Knox, J. B. Cross, V. Bakken, C. Adamo, J. Jaramillo, R. Gomperts, R. E. Stratmann, O. Yazyev, A. J. Austin, R. Cammi, C. Pomelli, J. W. Ochterski, R. L. Martin, K. Morokuma, V. G. Zakrzewski, G. A. Voth, P. Salvador, J. J. Dannenberg, S. Dapprich, A. D. Daniels, O. Farkas, J. B. Foresman, J. V. Ortiz, J. Cioslowski, and D. J. Fox, Gaussian, Inc., Wallingford CT, 2013.
- (4) N. S. Makarov, M. Drobizhev, A. Rebane, Two-photon absorption standards in the 550-1600 nm excitation wavelength range, *Opt. Express* 16 (2008), 4029.